Article:

Gordon, L.E., San Nicolas, R. and Provis, J.L. orcid.org/0000-0003-3372-8922 (2014) Chemical characterisation of metakaolin and fly ash based geopolymers during exposure to solvents used in carbon capture. International Journal of Greenhouse Gas Control , 27. pp. 255-266. ISSN 1750-5836

https://doi.org/10.1016/j.ijggc.2014.06.005

Please cite this paper as: Gordon, L.E.; San Nicolas, R.; Provis, J.L. "Chemical characterisation of metakaolin and fly ash based geopolymers during exposure to solvents used in carbon capture," *International Journal of Greenhouse Gas Control,* **2014,** *27*: 255-266. DOI 10.1016/j.ijggc.2014.06.005

Chemical characterisation of metakaolin and fly ash based geopolymers during exposure to solvents used in carbon capture

Laura E. Gordon[a,b], Rackel San Nicolas[a,b], John L. Provis[a,b,c]*

[a]*CO2CRC, University of Melbourne, Victoria 3010, Australia*
[b]*Department of Chemical & Biomolecular Engineering, University of Melbourne,*
Victoria 3010, Australia
[c]*Department of Materials Science and Engineering, University of Sheffield, Sheffield, S1 3JD,*
South Yorkshire, UK

** Corresponding author. Tel.: +44 (0)114-222-5490; fax:+44 (0) 114-222-5943.*
E-mail address:j.provis@sheffield.ac.uk.

Abstract

This paper presents an investigation into the chemical resistance of blended alkali activated aluminosilicate materials, specifically under exposure to two solvents used in post-combustion carbon capture, monoethanolamine (MEA) and potassium carbonate, as well as during immersion in distilled water. Geopolymers are formulated based on metakaolin and on fly ash as aluminosilicate precursors, with the addition of ground granulated blast furnace slag (GGBFS) as a source of Ca. The samples are subjected to mineralogical and chemical characterisation in this paper, with data obtained through leaching analysis and X-ray diffraction, supported by compressive strength data. Exposure to solvents generally results in significant alteration of the geopolymer microstructure. The zeolitic phases formed in undamaged metakaolin-based binders are reduced to undetectable levels after 28 days of solvent exposure, although the hydrosodalite formed in the fly ash binders does persist. Leaching analysis indicates that resistance to structural damage in MEA is quite high, due to the low solubility of Na and hydroxides upon immersion. K_2CO_3 solutions are aggressive towards geopolymers via alteration of the binder structure and dissolution of network-forming species (Si and Al), leading to the loss of binder strength. This is most marked in the fly ash/GGBFS formulations. Despite the low to intermediate level of Ca present in these geopolymer binders, significant formation of Ca-containing carbonate phases occurs upon exposure to K_2CO_3. The limited curing duration of the specimens tested here is certainly contributing to the degradation taking place under K_2CO_3 exposure, whereas the low water activity in the MEA solutions used means that bond hydrolysis in the aluminosilicate geopolymer framework is restricted, and the materials perform much better than in a more water-rich environment.

Keywords: Construction materials; process equipment; concrete; geopolymer; solvent processes

1. Introduction

Traditional cementing binders are formed via the hydration reactions of calcium silicate phases, whereas geopolymer concretes are synthesised by the alkali activation of aluminosilicates to form the binder. There is currently widespread research into the development of geopolymers and alkali activated systems (Provis 2014; Provis and van Deventer 2014), motivated not only by the beneficial technical properties of the material, such as thermal and chemical resistance, but also by the greatly reduced carbon emissions in geopolymer production relative to traditional cementing binders (McLellan et al. 2012). It is estimated that 5-8% of global anthropogenic carbon emissions are due to cement production (Olivier et al. 2012), driving research towards forming alternative low emissions binders as a viable commercial option (van Deventer et al. 2010; Juenger et al. 2011; van Deventer et al. 2012).

As a means of reducing the CO_2 emissions profiles of the global energy and cement industries, which are large point sources of CO_2, carbon capture and storage (CCS) processes and facilities are currently being trialed (Jenkins et al. 2012), with viability depending strongly on the costs involved. Post-combustion carbon capture solvent columns are generally constructed from stainless steel, as good mechanical performance and a high degree of chemical resistance are required from a column construction material. Geopolymer concretes are proposed to provide a durable, cost saving ‘green cement’ alternative structural material for the construction of large CCS facilities, with the aluminosilicate geopolymer chemistry suggested to provide the possibility of withstanding the harsh chemical environments found within these systems (Gordon et al. 2011) as the chemical resistance of geopolymers has long been promoted as a benefit of these materials (Davidovits 1991), and has been highlighted in laboratory testing over a number of years (Davidovits 1991; Bakharev 2005; Fernández-Jiménez et al. 2006; Duxson et al. 2007a; Sindhunata et al. 2008; Fernández-Jiménez and Palomo 2009; Temuujin et al. 2011).

There are many appealing aspects of geopolymer concretes which may make them suitable for use as a construction material in carbon capture facilities. Relative to traditional concreting systems based on ordinary Portland cement (OPC), geopolymers can offer as much as 80% reduction in CO_2 emissions (Duxson et al. 2007b) These materials also utilise industrial wastes such as fly ash as an integral binder component; fly ash is currently landfilled at a rate of several million tonnes p.a. in Australia alone, and hundreds of millions of tonnes p.a. worldwide, bringing appealing synergies if the material was to be used in carbon capture applications associated with coal-fired electricity generation.

Fly ash is a by-product from the combustion of coal in thermal power plants, whereas metakaolin is an industrial mineral product formed by the calcination of kaolinite clay. However, the use of metakaolin as the aluminosilicate source in geopolymer synthesis provides a relatively simpler model system for the study of geopolymers when compared to the multiphase and highly variable nature of industrial aluminosilicate wastes such as fly ash, In particular, metakaolin-based systems provide a more straightforward system to aid in understanding the mechanisms of reaction leading to binder formation, as well as resistance to chemical attack and consequently durability in service. This study builds new understanding of these properties by analysing the effects of exposure to the solvents used in post combustion carbon capture, on both fly ash and metakaolin based geopolymer systems. It is unlikely that metakaolin-based geopolymer concretes would be seriously considered for large-scale use in this type of application due to their generally high porosity, but they are valuable as a means of understanding the influence of the solvents on the aluminosilicate gel structure.

The chemical durability problems of traditional ordinary Portland cement based systems are generally caused by the degradative changes that occur in the calcium containing phases (Taylor 1997). Previous work in the analysis of the potential use of different types of concrete in CCS applications considered the exposure of OPC and OPC-based composite systems to the same carbon capture solvents that are analysed here (Gordon et al. 2011). Decalcification occurred upon exposure to MEA, and significant carbonation occurred upon exposure to K_2CO_3. However, the mechanisms controlling chemical resistance in an aluminosilicate geopolymeric gel will be expected to be different, based on the very different degree of cross-linking in the silicate binder gels (Duxson et al. 2007a; Abora et al. 2014).

This paper will describe the chemical characterisation of geopolymer paste samples during exposure to lean carbon capture solvents, through elemental analysis of the leaching solutions and X-ray diffractometry (XRD) of the pristine and leached materials. Lean solvents have been selected for analysis, rather than CO_2-loaded solvents, because it is more likely that concrete construction would be considered initially for use in the less chemically-aggressive parts of a carbon capture process, rather than in the more challenging environment of exposure to a rich solvent. Compressive strength data are presented to provide some insight into the influence of the leaching process on mechanical performance.

2. Materials and Methods

2.1. Sample formulations

The metakaolin used was sold under the brand name Metastar 402 by Imerys Minerals, UK. It has a BET surface area of 12.7 m^2/g and a mean particle size d_{50} of 1.58 µm (Duxson et al. 2006). The fly ash was from the Gladstone power station, Queensland, Australia and the ground granulated blast furnace slag (GGBFS) was obtained from Independent Cement & Lime, Australia. Table 1 presents the component oxide ratios for these materials.

A series of 32 geopolymer formulations were examined (Table 2). Of these, 15 were based on a mixture of metakaolin and ground granulated blast furnace slag (MK:GGBFS mass ratio 3:1) and 15 based on fly ash mixed with ground granulated blast furnace slag (FA:GGBFS mass ratio 2:1), along with a pure metakaolin-based binder and a pure fly ash-based binder. All mixes were activated with liquid sodium silicate activators, made by combining a commercial sodium silicate solution (Grade N®, PQ Australia, composition (mass basis):

SiO_2 28.7%, Na_2O 8.9%, H_2O 62.4%) with NaOH and Milli-Q water, to give the oxide ratios shown in Table 2. Table 3 summarises the parameters which were varied in each sample set in Table 2.

2.2 Analytical methodology

Leaching analysis was carried out using cylindrical sections of paste samples, which were cured under sealed conditions for 48 hours at 40°C and a further 5 days at room temperature (23±2°C) prior to exposure to aggressive conditions. A solid section of ~15 g weight was submerged in 200 mL of solvent: either 98% monoethanolamine (MEA), 2.5 M K_2CO_3, or Milli-Q grade purified water. An aliquot of 1 mL of solution was removed after 1, 3, 7, 14, 28 and 90 days. The volume of leachate removed was replenished with fresh solvent and a pH measurement taken at each sampling. The leachate samples were diluted 10× with 10 wt.% HCl solution for analysis by inductively coupled plasma-optical emission spectroscopy (ICP-OES) to determine the concentrations of Al, Si, Na and Ca present.

For compressive strength testing, mortar specimens of each formulation were made with the addition of sand at a 3:1 volume ratio of sand to aluminosilicate solids. These were sealed in 50 mm cubic moulds at 40 ^{o}C for 48 hours, then held at room temperature and maintained sealed, to match the curing regime used for the paste samples. After 7 and 28 days, they were analysed for compressive strength. Three replicate specimens were tested for each sample, and the mean results are reported.

Mortar cube samples were also submerged in the solvents (98% MEA, 2.5M K_2CO_3 and Milli-Q water) for 28 days, without replenishment of the solvent, before being analysed for compressive strength; again there were three replicates for each sample and the mean result is reported.

X-ray diffraction analysis was carried out on crushed paste samples after 90 days of exposure, on a Bruker D8 Advance using Cu Kα radiation, $\lambda = 1.5405$ Å. Traces were measured at a scan speed of 5s/step and a step size of 0.02°, from 5 to 55° 2θ.

3. Results and discussion

3.1. Leaching and mechanical strength

Figures 1 and 2 show the measured extent of leaching of both Si (Figure 1) and Al (Figure 2) from all of the metakaolin-based and fly ash-based geopolymer formulations in each of the three solvents. These plots do not show sample-specific data, but instead give an overall view of the leaching resistance of each binder as a function of the solvent used. There was high resistance to MEA, with generally <1% Si and Al leaching in this solvent during the test duration. However, there was notably increased leaching of matrix components induced by alkali attack on the matrix in both K_2CO_3 and H_2O. The pH value exceeded 12 after one day of exposure in all solvents, due to release of alkalis from the pore solution of the samples, and remained at this level throughout the duration of the study. The leaching of matrix components was rapid, with the majority of the leaching taking place within the first day of exposure to all solvents. There was then a further, very gradual release of Si and Al with increased solvent ingress into the binders over time, and this effect was more marked in the fly ash formulations than the metakaolin binders, probably due to the lower w/b ratios achievable in a mix design using spherical fly ash particles rather than plate-shaped metakaolin particles as the aluminosilicate source (Provis et al. 2010).

The main reason for the high degree of leaching observed here was that the pastes were quite immature at the point in time when they were first immersed in the solvents (i.e., 7 days of curing under sealed conditions at near-ambient temperature). This was designed to enable a comparative analysis between the dissolution of binder components within a realistic laboratory test time frame, as more mature geopolymer binders have been shown to display a much lower degree of leaching of binder components during extended exposure to alkaline solutions (Sindhunata et al. 2008; Temuujin et al. 2011). This is necessary in order to develop a scientific understanding of the influence of synthesis parameters on binder performance under these conditions, as more mature binders would be expected to show relatively less variation in nanostructure and microstructure after leaching due to the reduced influence of the solvent environment, and would thus be less instructive than the less-mature specimens investigated here.

An intermediate level of Ca content was provided to the binders studied here by the addition of granulated blast furnace slag (GGBFS). This is known to enhance the impermeability properties of the binder by the formation of a void filling, low-Ca, Al-substituted calcium silicate hydrate (C-(A)-S-H) gel in coexistence with the alkali aluminosilicate gel resulting from geopolymerisation (Kumar et al. 2010; Provis et al. 2012). The relatively low content and accessibility of calcium in the geopolymer binders is predicted to prevent the degradative effects of solvent-induced carbonation. Carbonation by gaseous CO_2-rich environments has been shown to be reasonably rapid in some alkali-activated binder systems (Puertas et al.

2006; Bernal et al. 2010), but the mechanism of carbonation in the fully saturated environments studied here, and its influence on the binder structure, are expected to differ significantly.

Previous studies of acid and alkali resistance in geopolymers found that mass and strength loss occurred through leaching, correlating with the increasing porosity of the binders through (Temuujin et al. 2011; Lloyd et al. 2012; McLellan et al. 2012) or alkali (Sindhunata et al. 2008; Temuujin et al. 2011) attack. The leaching of Fe, Al and Na was high in acidic solutions, and Si leaching dominated in alkaline conditions.

The trends displayed in Figure 1 show that the leaching of Si in K_2CO_3 in the fly ash-based systems occurred more readily relative to the metakaolin-based systems, while Al leaching (Figure 2) is significantly greater in water than in either of the carbon capture solvents used. Perera et al. (2006) showed that the release of alkali metal cations from both fly ash and metakaolin based geopolymers was high in distilled water when accompanied by hydroxide leaching, and the pH, both in that study and in our experiments, was found to be greater than 12 throughout the test period. It is possible that the presence of carbonate at this pH is suppressing the solubility of $Al(OH)_4^-$, most likely by increasing the ionic strength of the solution.

Figure 3 shows the total Si, Al, Na and Ca leached, expressed as a percentage of the total inventory of each element in the samples, after 90 days of exposure.

If each oxide ratio series is viewed separately (Table 3), Si leaching increases through the series with increasing SiO_2/Al_2O_3 ratio (2Na-4Na for MK/GGBFS and 18-22Na for FA/GGBFS) in all solvents. This is also accompanied by a loss in compressive strength (Figure 4). The strength loss is attributed to the reduced availability of Al for reaction, which is known to control the strength properties of geopolymers (Weng et al. 2005; Fernández-Jiménez et al. 2006; Duxson et al. 2007a). Aly *et al.* (2008) proposed that a lower degree of polymerisation occurs at higher Si/Al ratios, and supported this proposal using ^{29}Si and ^{27}Al magic angle spinning nuclear magnetic resonance (MAS NMR) spectroscopy: a reduced influence of Al on the average Si coordination sphere was observed, and XRD and infrared spectroscopic data also indicated a structural shift towards amorphous silica with increasing Si/Al ratio. This indicates that the correlation between reduced strength and increased leaching of Si is due to the reduced extent of geopolymerisation reactions within these immature binders, as the extent of incorporation of Si into the binder itself is not yet high.

However, the correlation between more marked strength loss and increased leaching does not follow for all of the binders. For example, the leaching extents observed in samples 7Na and 23Na are the lowest in their respective series (Figure 3), but unexposed strength was low in 7Na (~13 MPa) after 28 days of aging, and exposure to MEA resulted in catastrophic strength loss (Figure 4). The same trend is observed in sample 23Na (strengths of <5 MPa, no residual strength in water or K_2CO_3). This may be related to the low extent of reaction of the aluminosilicate precursors, as both of these specimens are formulated specifically to test the effect of a reduction in the Na_2O/SiO_2 ratio; i.e., a reduction in activator alkalinity, and thus reduced extent of interaction with the aluminosilicate particles during the geopolymerisation reaction. It is therefore necessary to consider this process to bring understanding of the formation, and subsequent degradation by leaching, of geopolymer binders.

Previous studies have considered the rate and extent of dissolution of fly ash in alkaline media, which is central to this discussion. Li *et al*. (2011) showed that the extent of fly ash dissolution in NaOH solutions was relatively low, even at high NaOH concentrations (6.0-13.4 M). In that study, the dissolution of Al occurred more readily than Si, shown by the variation of Si/Al ratio over time (Li et al. 2011) but in an earlier study (Pietersen et al. 1989), congruent dissolution was observed. It appears that the details of this process depend on the specific chemistry of the fly ash under analysis, and also the leaching environment used; Phair and van Deventer (2001) tested the leaching of Si and Al from a fly ash sourced from the same power station as the material used here, and found that the degree of incongruency of dissolution (favouring more rapid Al release) generally decreased with increasing NaOH concentration. Here, at the lowest alkali concentrations tested (sample 7Na in the fly ash system), it appears that the binder after 7 days of curing is sufficiently immature that the concentration of gel (which is the part of the material susceptible to solvent leaching) is low enough to give an apparently low extent of overall leaching, in parallel with poor strength performance. For the case of the metakaolin samples (particularly 13Na), the situation is broadly similar. Additionally, previous leaching studies have observed reprecipitation of aluminosilicate gels during leaching of geopolymers in alkaline solutions (Sindhunata et al. 2008), and this may also partially explain the low leaching rate found here when high strength loss and structural damage have occurred.

Where the Na_2O/SiO_2 ratio is increased (samples 7Na-9Na for MK/GGBFS and 23Na-27Na for FA/GGBFS), variation in water content was required to hold H_2O/Na_2O constant with the increase in alkalinity. As noted above, Sindhunata *et al.* (2008) observed reprecipitation of aluminosilicate species when geopolymers were exposed to highly alkaline solutions, but this effect was reduced marked at very high alkalinity. There is increased leaching of Si when increasing the Na_2O/SiO_2 ratio in the fly ash sample series (23Na-27Na, Figure 3e), which is assigned in part to the increased formation of geopolymer gel at higher alkalinity, and in part to the higher water content, which would be expected to increase porosity and permeability and thus increase alkali attack.

Correspondingly, the samples where the water content was the sole parameter varied (13Na-16Na and 28Na-32Na) do show a trend towards reduction in strength at increased water content (Figure 4). The generally increased leaching of Si follows in the fly ash formulations (28Na-32Na), Figure 3e. However, leaching remains low and follows no particularly apparent trend with respect to water content in the metakaolin binders; reprecipitation of aluminosilicate gels is likely to provide an explanation for this observation. The leaching of Al is significantly higher in water than in K_2CO_3. The samples with very low leaching of Al (28Na-31Na, Figure 3f) are those that have both high unexposed and residual strengths.

The amount of Na leached is higher than all the other ions for every formulation, which is related to the high mobility rate of those ions compared to the other ones studied, as Na is present largely in the pore solution of the materials, and in weakly associated charge-balancing sites (Lloyd et al. 2010). Further, the leaching of Na is significantly lower in MEA compared to H_2O and K_2CO_3, as MEA is a less effective solvent than aqueous environments for alkali hydroxides. For the fly ash formulations, no clear trends can be observed in the MEA solution. However in water and K_2CO_3 there is decreased leaching of Na with increased Na_2O/SiO_2 ratio in the fly ash sample series (23Na-27Na) which is contrary to the behaviour of Si and Al (Figure 3g) where increased leaching is attributed to the higher water content and assumed higher porosity through this series. The higher alkalinity of these systems results in greater production of geopolymer gel and so possibly the Na is chemically bound within the pore structure through the electrostatic interactions with the geopolymer matrix. Na is increasingly leached when the H_2O/SiO_2 ratio increases (28Na-32Na), due to the higher water content.

The significant observed extent of Ca leaching (Figure 3d,h) shows that a significant proportion of the Ca present is available for leaching by the solvent solutions. Previous work has shown that significant decalcification occurs in OPC, OPC/GGBFS and OPC/FA binders on exposure to MEA (Gordon et al. 2011), so these data show that the Ca-containing gels formed in these geopolymer systems seem to release Ca in a similar manner. X-ray diffraction data, presented below, show that in addition to the Ca present as dissolved species in the leaching solution, additional Ca is removed from the gel binder and precipitated in the formation of calcite ($CaCO_3$) on exposure to K_2CO_3, and also due to atmospheric carbonation in a few samples where the seal on the leaching vessel had been breached during sampling throughout the testing period.

3.2. X-ray diffraction

Figures 5-6, and the Supporting Information, show XRD traces for the metakaolin/GGBFS based binders, with separate figures focusing on each series of oxide ratios and their exposure under different conditions (Table 2), and compared to the binders of the same formulation which were aged at room temperature under sealed conditions for durations corresponding to the solvent exposure tests.

Figure 5 presents data for samples 2Na-4Na. The muscovite ($KAl_2(Si,Al)_4O_{10}(OH)_2$, PDF#58-2035) was present as an impurity in the metakaolin used, and reacts only slightly during geopolymer formation (Yip et al. 2008). The mixed carbonate - bicarbonate phase trona $Na_3(CO_3)(HCO_3)\cdot 2H_2O$ formed on the surface of the pure metakaolin sample 1Na and also on the surfaces of samples 1Na-4Na through atmospheric exposure, possibly in the initial curing stage when the samples were held at 40 °C for 48 hours as this phase is thermodynamically more stable at temperatures slightly higher than room temperature (Bernal et al. 2012). Pirssonite $CaNa_2(CO_3)\cdot 2(H_2O)$, formed by atmospheric carbonation, was also detected in samples 3Na (and thus is shown in the corresponding plots as 9Na and 14Na) and also in sample 12Na, but was not detected in these samples following solvent exposure. However, it has formed in sample 15Na following exposure to MEA, although this may also have been due to some atmospheric carbonation prior to or during XRD analysis.

A zeolite phase, faujasite (approximately $Na_2Al_2Si_{3.3}O_{10}\cdot 7H_2O$, PDF# 12-0228) has formed in all samples. At the highest SiO_2/Al_2O_3 ratio a Na-chabazite zeolite phase (approximately $NaAlSi_2O_6\cdot 3H_2O$, PDF# 19-1178) has also formed. Very little zeolite was detected in all samples following solvent exposure, with only small faujasite peaks detected in sample 3Na following exposure to H_2O. This appears to be related to the limited extent of zeolite formation observed after 7 days of curing (where the residual activator in the pores was washed out during immersion in water, effectively stopping the geopolymerisation/zeolite growth reaction), rather than via the removal of zeolitic phases during immersion. A study of accelerated aging of geopolymers (Lloyd 2009) showed that at 23°C there was no zeolite crystallisation in a metakaolin geopolymer for up to 3 months of aging. That study also considered the relationship between zeolite formation and strength retention in geopolymeric systems, concluding that the strongest correlation is between pore network stability and strength retention, rather than observing a direct link between zeolite evolution and geopolymer strength. Palomo et al. (1999) also exposed immature alkali activated metakaolin geopolymer to aggressive solutions, where the binders had been subjected to accelerated curing (85 °C) for just 2 days prior to exposure, and also found faujasite across a wide range of pH conditions, but not until at least 3 months of exposure in the samples immersed at high pH.

Zeolite formation within geopolymer binders is a complex process (Provis et al. 2005) and not yet fully understood. However, the formation of Na-chabazite along with faujasite in only sample 4Na (Figure 5a) is attributed to the increased Si/Al ratio of this sample. The high Si/Al ratio, reduced extent of geopolymerisation and alkali-rich pore solution conditions lead to the coexistence of these zeolitic phases (faujasite and chabazite), which is not observed in the formulations with less Si.

Solvent exposure in general inhibits the formation of zeolites compared to the unexposed samples, most likely due to the removal or dilution of the alkaline pore fluids required for ongoing reaction within the geopolymer gel. Exposure to MEA (Figure 5b) left muscovite as the only crystalline phase observed in the samples, while the amorphous 'hump' characteristic of the disordered aluminosilicate geopolymer framework (Provis et al. 2005) remains intact. This is in good agreement with the low level of leaching of both Si and Al found on exposure to MEA in all samples.

Exposure to water (Figure 5c) has also hindered the development of zeolitic phases through the dilution of the pore solution, and some carbonation, evident via the formation of crystalline calcite ($CaCO_3$, PDF #05-0586) occurred in samples 2Na and 3Na after exposure to water and K_2CO_3, showing that calcium is available for reaction with the atmosphere. This is in good agreement with the high leachability of Ca as observed in all solvents (Figure 3d). No zeolitic phases form during exposure to K_2CO_3 (Figure 5d), apart from a small amount of faujasite detected in samples 2Na and 3Na, which also forms in these formulations following exposure to water (Figure 5c).

Figure 6, which shows XRD data for the sample series with increasing Na_2O/SiO_2 ratio, demonstrates the formation of faujasite in samples 8Na and 9Na. No zeolitic phases have formed in sample 7Na (Figure 6a), which has the lowest Na_2O content; the lower extent of reaction of the aluminosilicate precursor phases in this system will affect the availability of species for zeolite crystallisation. Additionally, in this sample there was also a reduction in water content in order to achieve the Na_2O/SiO_2 ratio required, and this too may be significant in inhibiting the formation of zeolites, as steric restrictions may reduce the growth of germ nuclei which lead to the formation of crystalline zeolites (Barrer 1981; Provis et al. 2005). Sample 7Na also shows a small degree of atmospheric carbonation, seen through the formation of aragonite, a metastable polymorph of $CaCO_3$.

Following exposure to solvents, a significant quantity of faujasite develops only in 8Na after exposure to MEA (Figure 6b) and water (Figure 6c). A smaller quantity of faujasite is seen in the 9Na formulation exposed to water, and slight traces in 9Na following exposure to K_2CO_3 (Figure 6d). Significant calcite formation is again observed during K_2CO_3 exposure (Figure

6d) through decalcification, and kalcinite ($KHCO_3$, PDF # 12-0297) has also formed in all K_2CO_3 exposed samples through the reaction of K_2CO_3 with CO_2 and H_2O. Corresponding data and additional discussion related to the metakaolin sample series with increasing H_2O/SiO_2 ratios are presented as Supporting Information (Figure S1 and associated text). These data show the formation of zeolites in each sample, although their prevalence is reduced by K_2CO_3 exposure, which appears to hinder the structural evolution and crystallisation of the zeolites.

The XRD data for the fly ash-based formulations are presented in Figures 7-8 and in the Supporting Information, again divided by oxide ratio series as outlined in Table 2. In these samples, a basic Na-sodalite phase (approximately, $1.08Na_2O{\cdot}Al_2O_3{\cdot}1.68SiO_2{\cdot}1.8H_2O$, PDF# 31-1271) was formed; this is a feldspathoid structure, closely related to zeolites, and appears to be present in all samples regardless of solvent exposure. Sample 17Na, the pure fly ash binder, also contains trona ($Na_3(CO_3)(HCO_3){\cdot}2H_2O$) as a product of slight atmospheric carbonation. Also present in all of the fly ash based formulations were the unreactive phases supplied by the fly ash, being quartz and mullite.

Figure 7 shows the data for the sample series with increasing SiO_2/Al_2O_3 ratio. The formation of basic sodalite appears to reduce as the Si content increases, likely due to the reduction in Al available for crystallisation, as this phase forms with $SiO_2/Al_2O_3 = 2$ and so requires high Al availability for crystallisation. The sodalite appears to be largely unaffected by exposure to MEA (Figure 7b). Si and Al leaching was also low for the fly ash formulations immersed in MEA (Figures 1 and 2), and residual strength on exposure to solvents was high (Figure 4). It therefore seems that for the fly ash formulations, 28 days of exposure to MEA has not significantly altered the expected path of microstructural development, with the slight losses in strength attributed to alkali attack on the framework.

The basic sodalite phase also develops in almost all samples following exposure to water (Figure 7c), but in concentrations again decreasing though the sample series. However, sample 18Na showed instead the formation of a faujasite phase as the main zeolitic product, similar to the fly ash-only sample 17Na. Sample 18Na had the lowest Si/Al ratio of the samples in this series. However, faujasite was not formed in the 18Na sample subjected to other immersion conditions, so its formation here may be due to the effectively increased water content on immersion, and the effect of the subsequent diffusion of the contents of the pore solution out into the leaching solution. Exposure to water is also accompanied by a significant amount of carbonation, with the formation of calcite in all samples of the fly ash-slag series.

A small amount of sodalite was also formed on exposure to K_2CO_3 (Figure 7d). Carbonation also occurred in all samples exposed to K_2CO_3 with the formation of calcite $CaCO_3$ (PDF# 47-1743) through decalcification and kalcinite, $KHCO_3$ (PDF# 12-0292) through reaction of K_2CO_3, CO_2 and H_2O. Some crystalline K_2CO_3 (PDF# 70-0292) also precipitated in all samples. The high leachability of Na and Si in K_2CO_3 (Figure 3) resulted in total strength loss after 28 days of solvent exposure (Figure 4), and this is consistent with the notable reduction in the amorphous ‘hump’ corresponding to the geopolymer gel in this leaching environment in particular (Figure 7d). The microstructural development has been significantly affected following 28 days of exposure to K_2CO_3, but despite this the mechanism of zeolite formation found in the unexposed samples still persists, although to a lesser extent due to the leaching processes taking place.

The XRD data for the series with increasing Na_2O/SiO_2 ratio are given in Figure 8. In the unexposed samples (Figure 8a), basic sodalite is more prominent with increasing Na content, with the exception of sample 27Na. In this formulation, the hydroxide and water contents are highest, and there is no trace of sodalite, but faujasite has formed instead. In sample 23Na, where hydroxide and water contents are low, no zeolitic phase has formed. Again, there is very little effect on the microstructure induced by exposure to MEA (Figure 8b) or water (Figure 8c). The same zeolites as in the unexposed samples, faujasite (in 27Na) and basic sodalite (in 24Na-26Na), have again developed (but to a lesser extent than in the unexposed samples) after exposure to K_2CO_3 (Figure 8d).

The XRD data for the series with increasing H_2O/SiO_2 ratio are shown in the Supporting Information. Basic sodalite was formed in all of the unexposed samples, and there appears to be very little difference in the crystalline phases formed, other than calcite formation in all samples, and slight suppression of crystallisation by K_2CO_3 immersion. This series had the highest unexposed and also residual strengths upon exposure after 28 days of immersion, and it appears that these five samples have the least alteration in crystallographic structure among those studied.

3.3 Implications

The specimens tested here show notable degradation under exposure to carbon capture solvents, and as such would not be directly useful in applications where they are brought into immediate contact with these solvents in service. However, this was a part of the design of this study, which is in effect an accelerated test to simulate a worst-case leaching scenario. The resistance of geopolymers to alkali attack and carbonation would certainly be higher if more mature binders were tested, but the aim of this study has been to elucidate the degradation mechanisms through induction of artificially rapid degradation processes. The key to geopolymer concrete durability in carbon capture applications will be the development of low porosity and high tortuosity of the pore structure, in order to reduce the accessibility of the key binder phases. A forthcoming study will directly address the pore network geometry of these binder systems, and provide further insight into this important issue. In any case, the results of this study show that the resistance of geopolymers to attack by aqueous K_2CO_3 is not as high as was predicted based upon nanostructural arguments, and this solvent does cause significant damage to the aluminosilicate geopolymer framework.

4. Conclusions

Alkali activated geopolymer concretes may provide a cost saving alternative construction material for use in place of large stainless steel vessels in carbon capture facilities. This study was based around the study of immature and relatively porous binders, in order to best understand the mechanism of chemical attack on geopolymers during exposure to carbon capture solvents. Leaching occurred rapidly, within one day of immersion, due to the release of alkalis from the pore solution and attack on loosely bound Si and Al species within these immature binders. Resistance to MEA is highest among the solvents tested, with low solubility of Na in this solvent.

The microstructural development of the metakaolin/slag geopolymer formulations was more significantly affected by solvent immersion than was the structure of the fly ash/slag geopolymers. Solvent immersion seems to suppress the formation of faujasite in the metakaolin/slag binders, and the residual strength of these binders is relatively low. However, the formation of basic sodalite, which is the predominant crystalline phase observed in the fly ash/slag formulations, is much less influenced by solvent immersion, particularly in the case of immersion in MEA or water, where the 28 day residual strength is high. The reduced extent of binder development observed on exposure to K_2CO_3 (evidenced by the lower degree of zeolite formation and also the dissolution of much of the amorphous geopolymer gel phase), along with the effects of significant carbonation does, in the majority of cases, caused catastrophic strength failure of the matrix on exposure to K_2CO_3.

5. Acknowledgements

The authors acknowledge the funding provided by the Australian Government through its CRC Program for this CO2CRC research project, and the salary support of JLP provided through the Discovery Grants program via APD and DORA Fellowships.

6. References

Abora, K., Beleña, I., Bernal, S.A., Dunster, A., Nixon, P.A., Provis, J.L., Tagnit-Hamou, A. and Winnefeld, F. (2014). Durability and testing - Chemical matrix degradation processes. in: Alkali-Activated Materials: State-of-the-Art Report, RILEM TC 224-AAM. Eds. J.L. Provis and J.S.J. van Deventer. Dordrecht, Springer/RILEM**:** 177-221.

Aly, Z., Vance, E.R., Perera, D.S., Hanna, J.V., Griffith, C.S., Davis, J. and Durce, D. (2008). "Aqueous leachability of metakaolin-based geopolymers with molar ratios of Si/Al=1.5-4." Journal of Nuclear Materials **378**(2): 172-179.

Bakharev, T. (2005). "Resistance of geopolymer materials to acid attack." Cement and Concrete Research **35**(4): 658-670.

Barrer, R.M. (1981). "Zeolites and their synthesis." Zeolites **1**(3): 130-140.

Bernal, S.A., Mejía de Gutiérrez, R., Provis, J.L. and Rose, V. (2010). "Effect of silicate modulus and metakaolin incorporation on the carbonation of alkali silicate-activated slags." Cement and Concrete Research **40**(6): 898-907.

Bernal, S.A., Provis, J.L., Brice, D.G., Kilcullen, A., Duxson, P. and van Deventer, J.S.J. (2012). "Accelerated carbonation testing of alkali-activated binders significantly underestimates service life: The role of pore solution chemistry." Cement and Concrete Research **42**(10): 1317-1326.

Davidovits, J. (1991). "Geopolymers - Inorganic polymeric new materials." Journal of Thermal Analysis **37**(8): 1633-1656.

Duxson, P., Fernandez-Jimenez, A., Provis, J.L., Lukey, G.C., Palomo, A. and van Deventer, J.S.J. (2007a). "Geopolymer technology: the current state of the art." Journal of Materials Science **42**(9): 2917-2933.

Duxson, P., Lukey, G.C. and van Deventer, J.S.J. (2006). "Thermal evolution of metakaolin geopolymers: Part 1 - Physical evolution." Journal of Non-Crystalline Solids **352**(52-54): 5541-5555.

Duxson, P., Provis, J.L., Lukey, G.C. and Van Deventer, J.S.J. (2007b). "The role of inorganic polymer technology in the development of 'green concrete'." Cement and Concrete Research **37**(12): 1590-1597.

Fernández-Jiménez, A. and Palomo, A. (2009). Chemical durability of geopolymers. in: Geopolymers: Structure, Processing, Properties and Industrial Applications. Eds. J.L. Provis and J.S.J. van Deventer. Cambridge, UK, Woodhead**:** 167-193.

Fernández-Jiménez, A., Palomo, A., Sobrados, I. and Sanz, J. (2006). "The role played by the reactive alumina content in the alkaline activation of fly ashes." Microporous and Mesoporous Materials **91**(1-3): 111-119.

Gordon, L.E., Provis, J.L. and van Deventer, J.S.J. (2011). "Durability of fly ash/GGBFS based geopolymers exposed to carbon capture solvents." Advances in Applied Ceramics **110**(8): 446-452.

Jenkins, C.R., Cook, P.J., Ennis-King, J., Undershultz, J., Boreham, C., Dance, T., de Caritat, P., Etheridge, D.M., Freifeld, B.M., Hortle, A., Kirste, D., Paterson, L., Pevzner, R., Schacht, U., Sharma, S., Stalker, L. and Urosevic, M. (2012). "Safe storage and effective monitoring of CO_2 in depleted gas fields." Proceedings of the National Academy of Sciences of the United States of America **109**(2): E35-E41.

Juenger, M.C.G., Winnefeld, F., Provis, J.L. and Ideker, J.H. (2011). "Advances in alternative cementitious binders." Cement and Concrete Research **41**(12): 1232-1243.

Kumar, S., Kumar, R. and Mehrotra, S.P. (2010). "Influence of granulated blast furnace slag on the reaction, structure and properties of fly ash based geopolymer." Journal of Materials Science **45**(3): 607-615.

Li, C., Li, Y., Sun, H. and Li, L. (2011). "The composition of fly ash glass phase and its dissolution properties applying to geopolymeric materials." Journal of the American Ceramic Society **94**(6): 1773-1778.

Lloyd, R.R. (2009). Accelerated ageing of geopolymers. in: Geopolymers: Structure, Processing, Properties and Industrial Applications. Eds. J.L. Provis and J.S.J. van Deventer. Cambridge, UK, Woodhead**:** 139-166.

Lloyd, R.R., Provis, J.L. and van Deventer, J.S.J. (2010). "Pore solution composition and alkali diffusion in inorganic polymer cement." Cement and Concrete Research **40**(9): 1386-1392.

Lloyd, R.R., Provis, J.L. and van Deventer, J.S.J. (2012). "Acid resistance of inorganic polymer binders. 1. Corrosion rate." Materials and Structures **45**(1-2): 1-14.

McLellan, B.C., Corder, G.D., Giurco, D.P. and Ishihara, K.N. (2012). "Renewable energy in the minerals industry: a review of global potential." Journal of Cleaner Production **32**: 32-44.

Olivier, J.G.J., Janssens-Maenhout, G. and Peters, J.A.H.W. (2012). Trends in global CO_2 emissions; 2012 Report. The Hague, Netherlands, PBL Netherlands Environmental Assessment Agency**:** 40 pp.

Palomo, A., Blanco-Varela, M.T., Granizo, M.L., Puertas, F., Vazquez, T. and Grutzeck, M.W. (1999). "Chemical stability of cementitious materials based on metakaolin." Cement and Concrete Research **29**(7): 997-1004.

Perera, D.S., Vance, E.R., Aly, Z., Davis, J. and Nicholson, C.L. (2006). Immobilization of Cs and Sr in geopolymers with Si/Al molar ratio of ∼2. in: Environmental Issues and Waste Management Technologies in the Ceramic and Nuclear Industries XI (Ceramic Transactions Vol. 176), John Wiley & Sons**:** 91-96.

Phair, J.W. and van Deventer, J.S.J. (2001). "Effect of silicate activator pH on the leaching and material characteristics of waste-based inorganic polymers." Minerals Engineering **14**(3): 289-304.

Pietersen, H.S., Fraay, A.L.A. and Bijen, J.M. (1989). Reactivity of fly ash at high pH. 1989 Materials Research Society Fall Meeting (MRS Proceedings Vol. 178), Boston, MA, Cambridge University Press.

Provis, J.L. (2014). "Geopolymers and other alkali activated materials - Why, how, and what?" Materials and Structures **47**(1): 11-25.

Provis, J.L., Duxson, P. and van Deventer, J.S.J. (2010). "The role of particle technology in developing sustainable construction materials." Advanced Powder Technology **21**(1): 2-7.

Provis, J.L., Lukey, G.C. and van Deventer, J.S.J. (2005). "Do geopolymers actually contain nanocrystalline zeolites? A reexamination of existing results." Chemistry of Materials **17**(12): 3075-3085.

Provis, J.L., Myers, R.J., White, C.E., Rose, V. and van Deventer, J.S.J. (2012). "X-ray microtomography shows pore structure and tortuosity in alkali-activated binders." Cement and Concrete Research **42**(6): 855-864.

Provis, J.L. and van Deventer, J.S.J., Eds. (2014). Alkali-Activated Materials: State-of-the-Art Report, RILEM TC 224-AAM. Dordrecht, Springer/RILEM.

Puertas, F., Palacios, M. and Vazquez, T. (2006). "Carbonation process of alkali-activated slag mortars." Journal of Materials Science **41**(10): 3071-3082.

Sindhunata, Provis, J.L., Lukey, G.C., Xu, H. and van Deventer, J.S.J. (2008). "Structural evolution of fly ash based geopolymers in alkaline environments." Industrial & Engineering Chemistry Research **47**(9): 2991-2999.

Taylor, H.F.W. (1997). Cement Chemistry, 2nd Ed. London, UK, Thomas Telford.

Temuujin, J., Minjigmaa, A., Lee, M., Chen-Tan, N. and van Riessen, A. (2011). "Characterisation of class F fly ash geopolymer pastes immersed in acid and alkaline solutions." Cement & Concrete Composites **33**(10): 1086-1091.

van Deventer, J.S.J., Provis, J.L. and Duxson, P. (2012). "Technical and commercial progress in the adoption of geopolymer cement." Minerals Engineering **29**: 89-104.

van Deventer, J.S.J., Provis, J.L., Duxson, P. and Brice, D.G. (2010). "Chemical research and climate change as drivers in the commercial adoption of alkali activated materials." Waste and Biomass Valorization **1**(1): 145-155.

Weng, L.Q., Sagoe-Crentsil, K., Brown, T. and Song, S.H. (2005). "Effects of aluminates on the formation of geopolymers." Materials Science and Engineering B-Solid State Materials for Advanced Technology **117**(2): 163-168.

Yip, C.K., Provis, J.L., Lukey, G.C. and van Deventer, J.S.J. (2008). "Carbonate mineral addition to metakaolin-based geopolymers." Cement & Concrete Composites **30**(10): 979-985.

Table 1. Compositions of aluminosilicate sources; wt.% as oxides, determined by X-ray fluorescence. LOI is loss on ignition at 1000 °C.

	Metakaolin	**Fly ash**	**GGBFS**
SiO_2	52.8	45.5	32.9
Al_2O_3	39.2	27.8	13.2
CaO	0.1	5.6	40.1
Na_2O	0.0	0.3	0.3
K_2O	2.7	0.5	0.3
Fe_2O_3	0.8	11.2	0.3
MgO	0.2	1.4	6.0
P_2O_5	0.1	0.5	0.0
SO_3	0.0	0.2	3.5
TiO_2	0.0	1.4	0.7
MnO	0.0	0.2	0.0
LOI	1.2	2.7	1.2

Table 2. Component molar oxide ratios, NaOH concentrations and water/binder ratios (w/b; ‘binder’ is defined as the solid aluminosilicate precursor) of the geopolymer formulations tested.

Solid aluminosilicate	**ID**	**SiO_2/Al_2O_3**	**Na_2O/SiO_2**	**H_2O/Na_2O**	**NaOH (M)**	**w/b**
MK	1Na	3.0	0.5	13.0	6.9	0.44
MK:GGBFS 3:1	2Na	3.0	0.5	13.0	7.2	0.44
MK:GGBFS 3:1	3Na	3.3	0.5	13.0	6.9	0.44
MK:GGBFS 3:1	4Na	3.6	0.5	13.0	6.6	0.45
MK:GGBFS 3:1	7Na	3.3	0.33	13.0	6.0	0.37
MK:GGBFS 3:1	8Na	3.3	0.4	13.0	6.5	0.40
MK:GGBFS 3:1	9Na	3.3	0.5	13.0	6.9	0.44
MK:GGBFS 3:1	12Na	3.3	0.5	11.0	8.2	0.40
MK:GGBFS 3:1	13Na	3.3	0.5	12.0	7.5	0.42
MK:GGBFS 3:1	14Na	3.3	0.5	13.0	6.9	0.44
MK:GGBFS 3:1	15Na	3.3	0.5	14.0	6.4	0.46
MK:GGBFS 3:1	16Na	3.3	0.5	15.0	6.0	0.48
FA	17Na	3.33	0.45	8.0	10.6	0.32
FA:GGBFS 2:1	18Na	3.1	0.45	8.0	12.2	0.32
FA:GGBFS 2:1	19Na	3.2	0.45	8.0	12.0	0.32
FA:GGBFS 2:1	20Na	3.33	0.45	8.0	11.7	0.33
FA:GGBFS 2:1	21Na	3.4	0.45	8.0	11.6	0.33
FA:GGBFS 2:1	22Na	3.5	0.45	8.0	11.4	0.33
FA:GGBFS 2:1	23Na	3.33	0.30	8.0	10.3	0.24
FA:GGBFS 2:1	24Na	3.33	0.36	8.0	10.9	0.27
FA:GGBFS 2:1	25Na	3.33	0.45	8.0	11.7	0.33
FA:GGBFS 2:1	26Na	3.33	0.6	8.0	12.1	0.36
FA:GGBFS 2:1	27Na	3.33	0.9	8.0	12.7	0.42
FA:GGBFS 2:1	28Na	3.33	0.45	7.0	13.4	0.27
FA:GGBFS 2:1	29Na	3.33	0.45	8.0	11.7	0.33
FA:GGBFS 2:1	30Na	3.33	0.45	9.0	10.4	0.33
FA:GGBFS 2:1	31Na	3.33	0.45	10.0	9.4	0.35
FA:GGBFS 2:1	32Na	3.33	0.45	11.0	8.5	0.37

[a] Samples shaded in grey are the same mix (one in the metakaolin-based sample set and one in the fly ash-based sample set), replicated and renumbered each time in the sample listing to place this composition in the correct position in the series in which each of the synthesis parameters was varied.

Table 3. Summary of sample series and the parameters varied in each.

Series	Aluminosilicate source	Parameter
2Na-4Na	Metakaolin-slag	Increasing SiO_2/Al_2O_3
7Na-9Na	Metakaolin-slag	Increasing Na_2O/SiO_2 (and w/b)
12Na-16Na	Metakaolin-slag	Increasing w/b
18Na-22Na	Fly ash-slag	Increasing SiO_2/Al_2O_3
23Na-27Na	Fly ash-slag	Increasing Na_2O/SiO_2 (and w/b)
28Na-32Na	Fly ash-slag	Increasing w/b

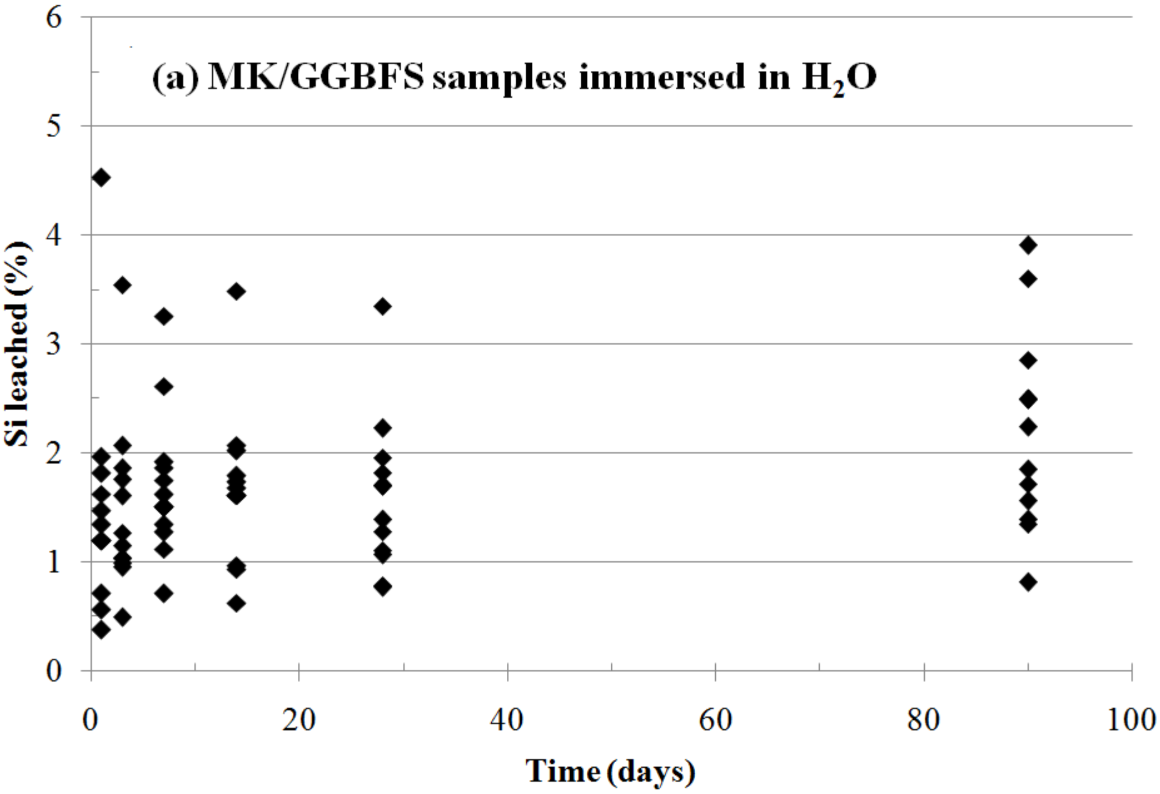
(a) MK/GGBFS samples immersed in H_2O
Si leached (%)
Time (days)
0
1
2
3
4
5
6
0
20
40
60
80
100

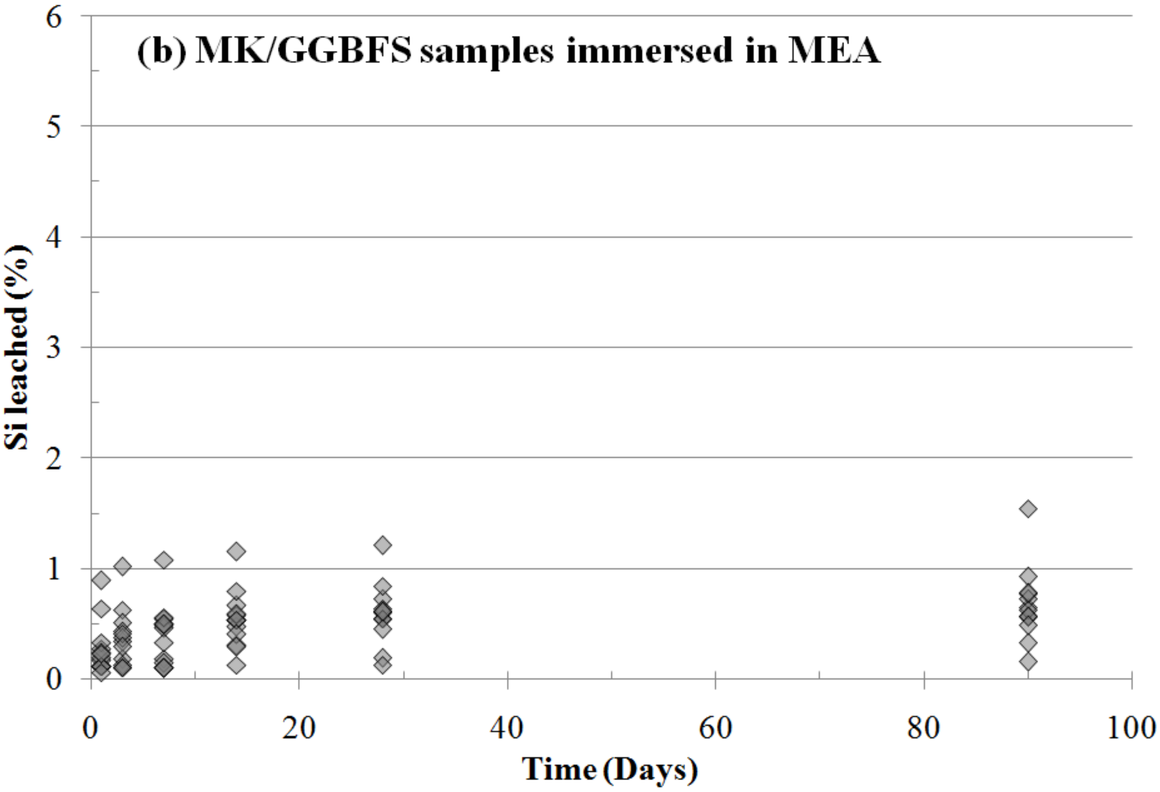
(b) MK/GGBFS samples immersed in MEA
Si leached (%)
Time (Days)
0
1
2
3
4
5
6
0
20
40
60
80
100

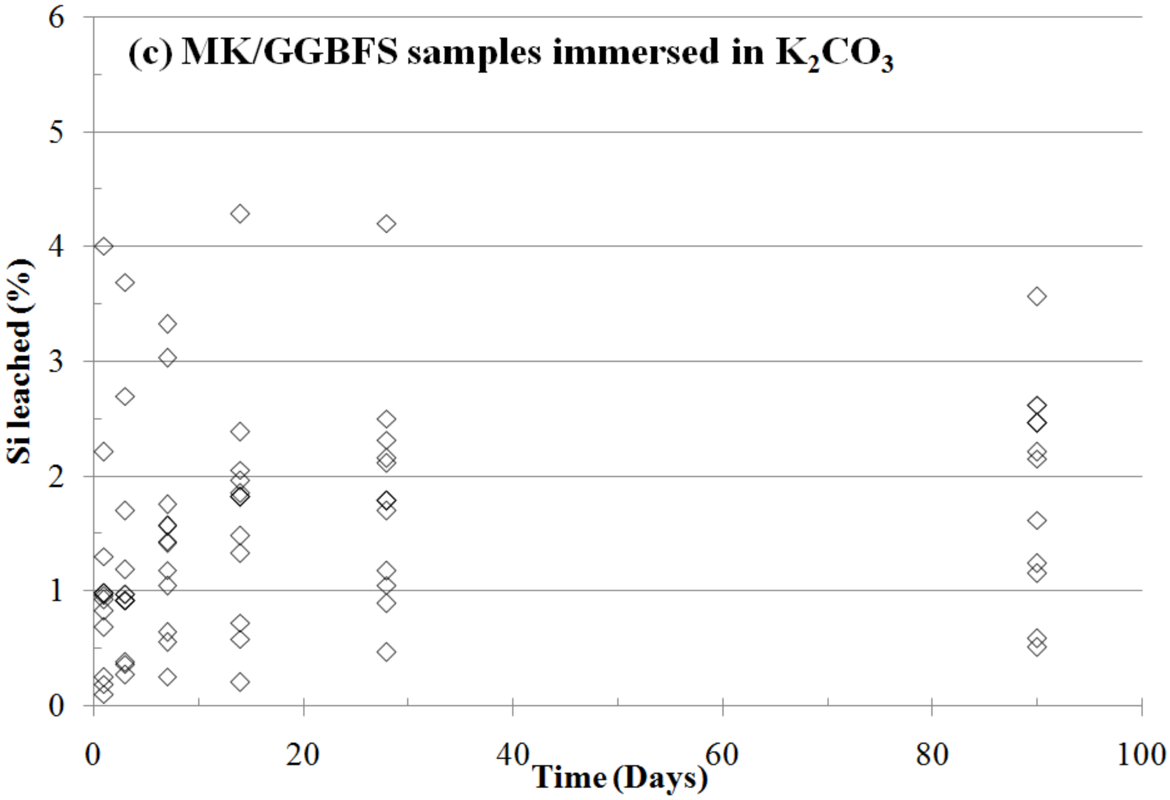
(c) MK/GGBFS samples immersed in K_2CO_3
Si leached (%)
Time (Days)
0
1
2
3
4
5
6
0
20
40
60
80
100

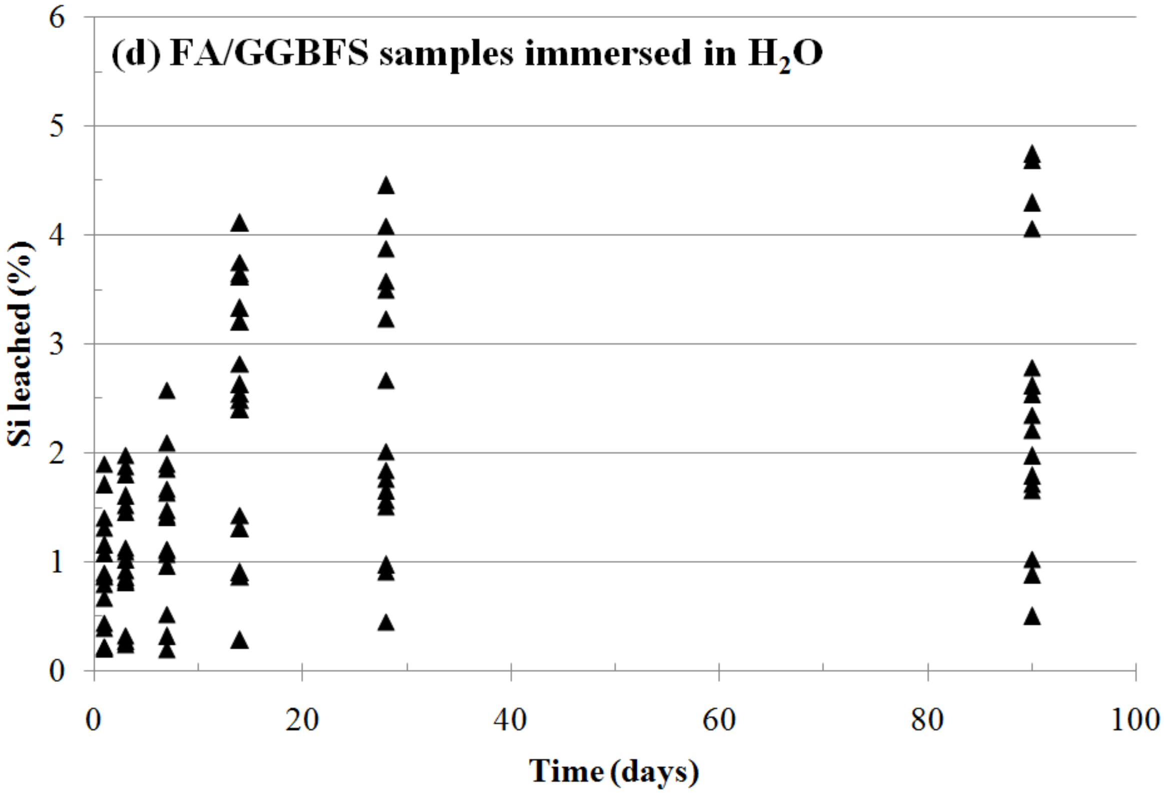
(d) FA/GGBFS samples immersed in H_2O
Si leached (%)
Time (days)
0
1
2
3
4
5
6
0
20
40
60
80
100

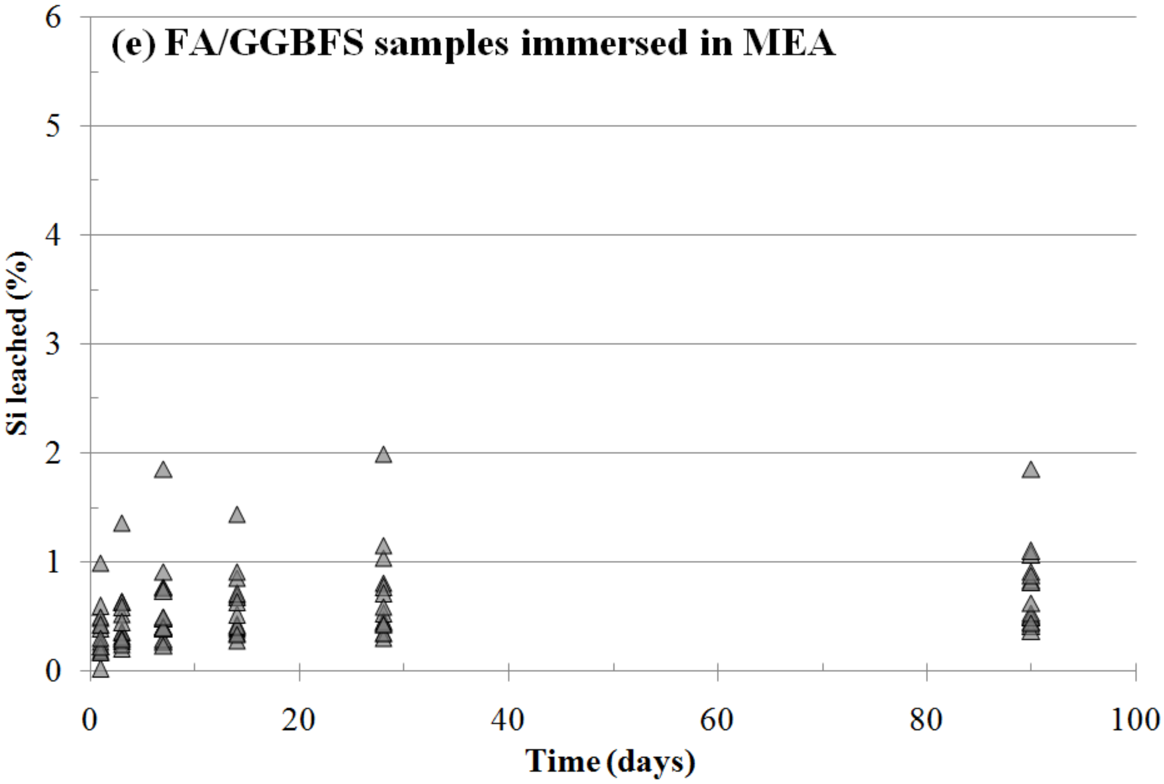
(e) FA/GGBFS samples immersed in MEA
Si leached (%)
Time (days)
0
1
2
3
4
5
6
0
20
40
60
80
100

639

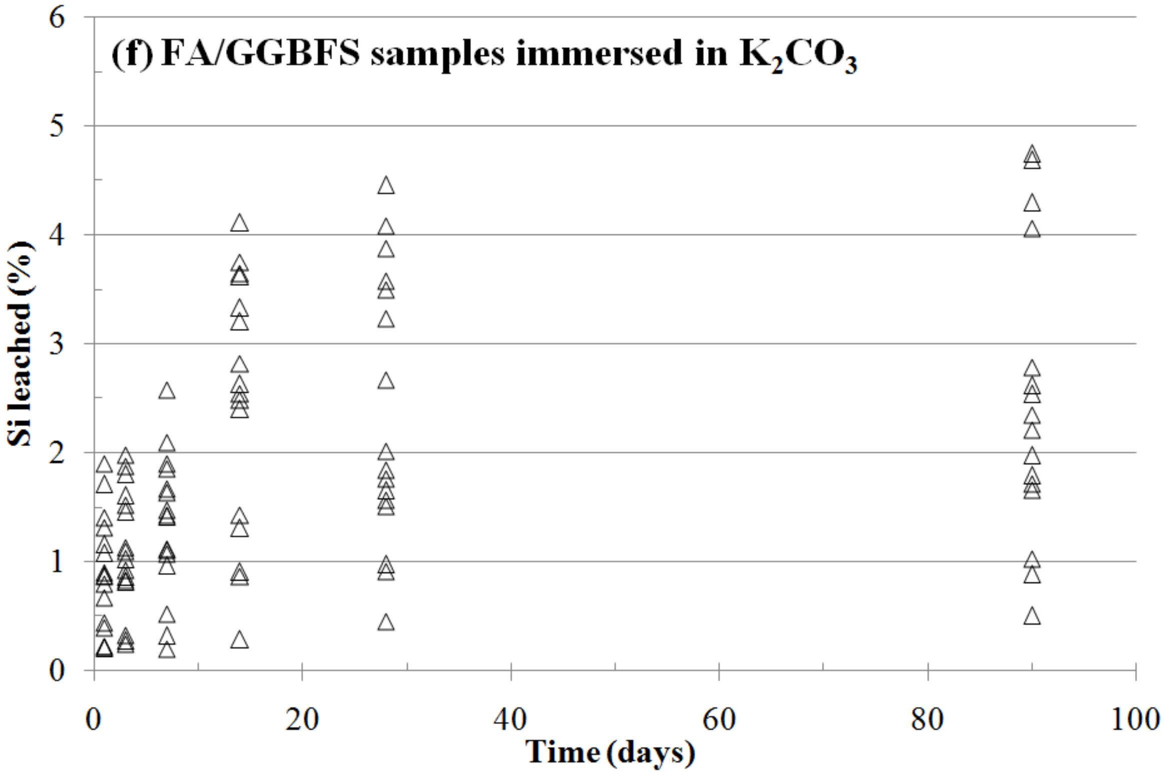
(f) FA/GGBFS samples immersed in K_2CO_3
Si leached (%)
Time (days)
0
1
2
3
4
5
6
0
20
40
60
80
100

640

641 Figure 1. Leaching of Si from (a, b, c) the MK/GGBFS binders and (d, e, f) FA/GGBFS
642 binders during 90 days of solvent exposure, (a, d) H_2O, (b, e) MEA, (c, f) K_2CO_3

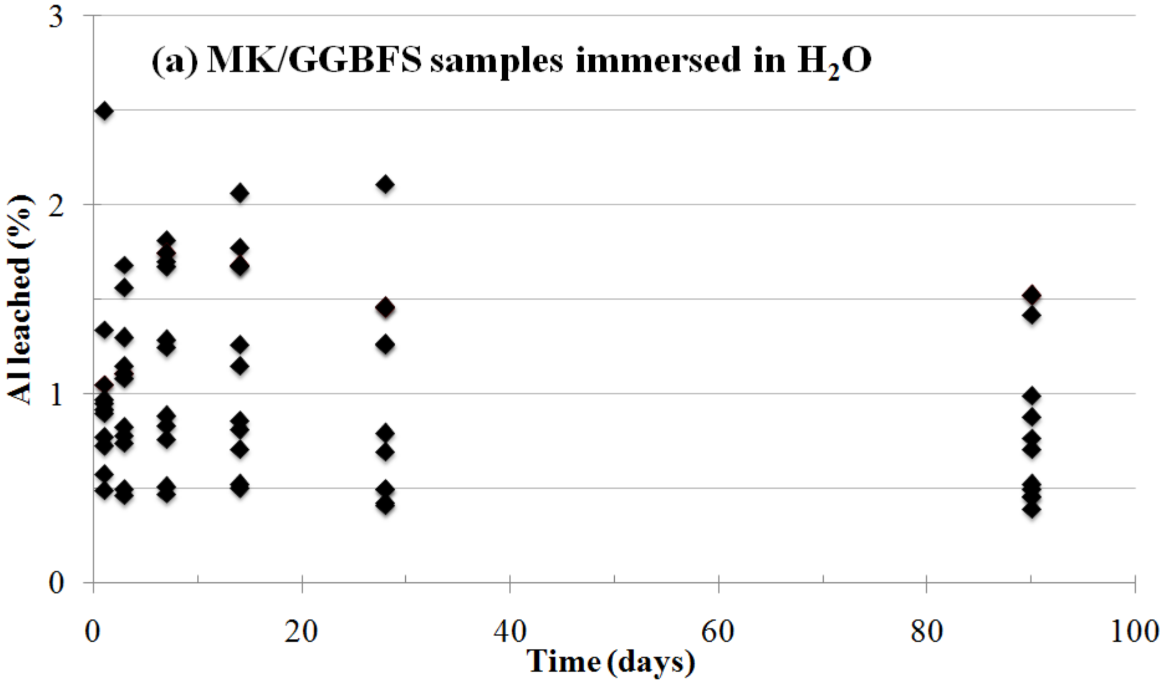

643

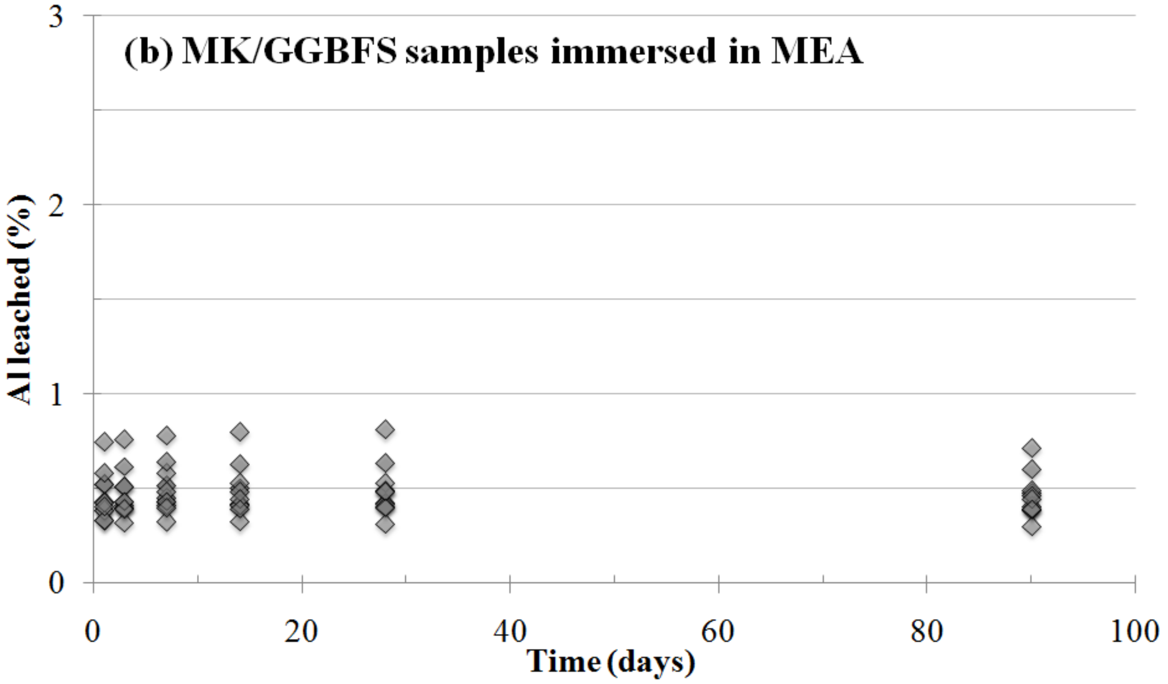

644

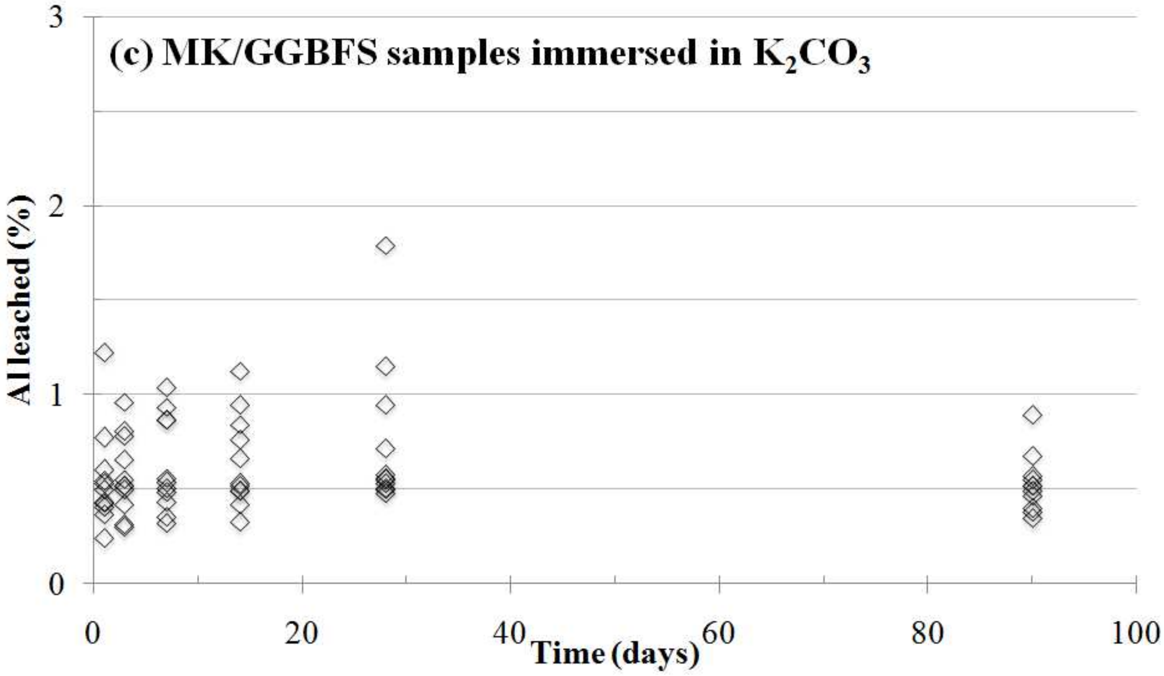
(c) MK/GGBFS samples immersed in K_2CO_3
Al leached (%)
Time (days)
0
1
2
3
0
20
40
60
80
100

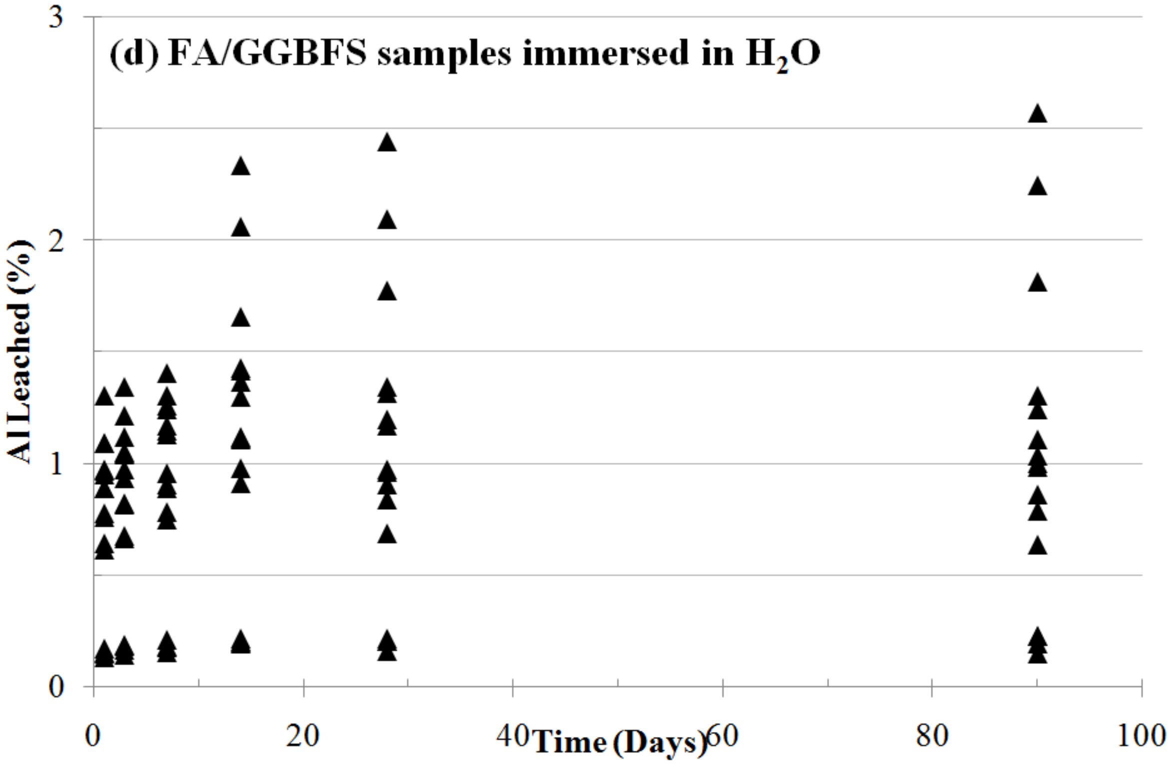
(d) FA/GGBFS samples immersed in H_2O
Al Leached (%)
3
2
1
0
0
20
40
60
80
100
Time (Days)

648

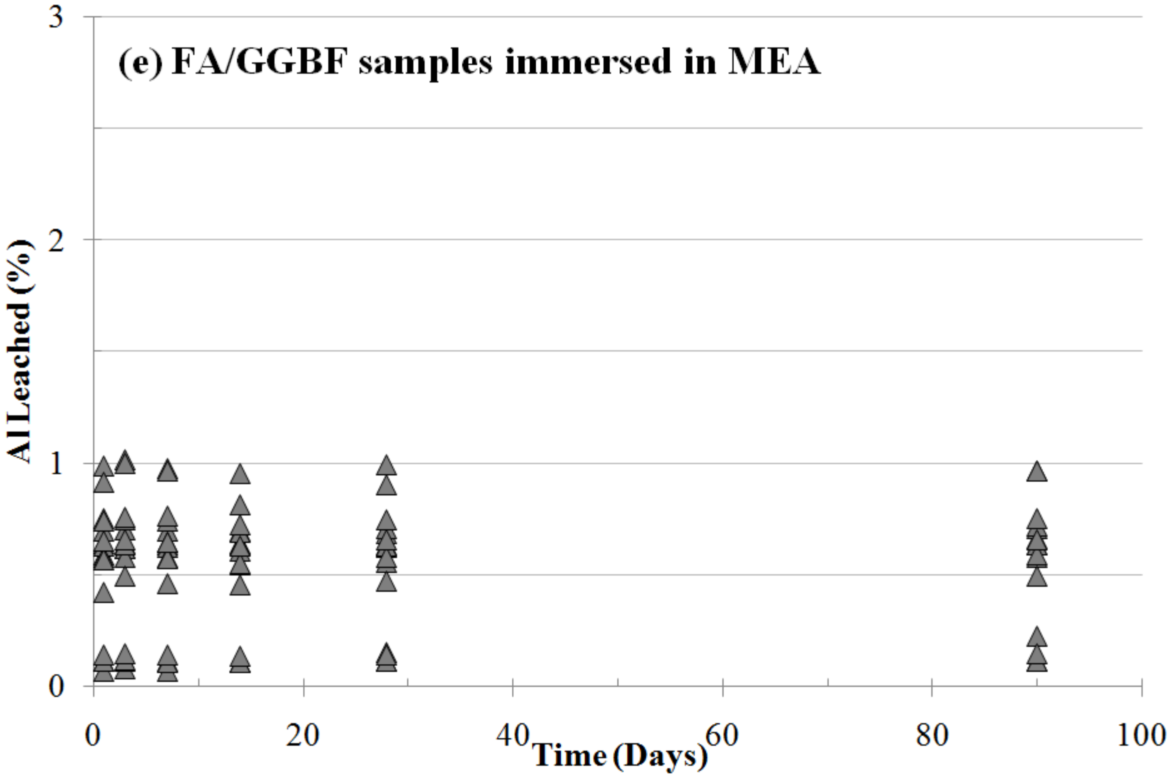
(e) FA/GGBF samples immersed in MEA
Al Leached (%)
3
2
1
0
0
20
40
60
80
100
Time (Days)

649

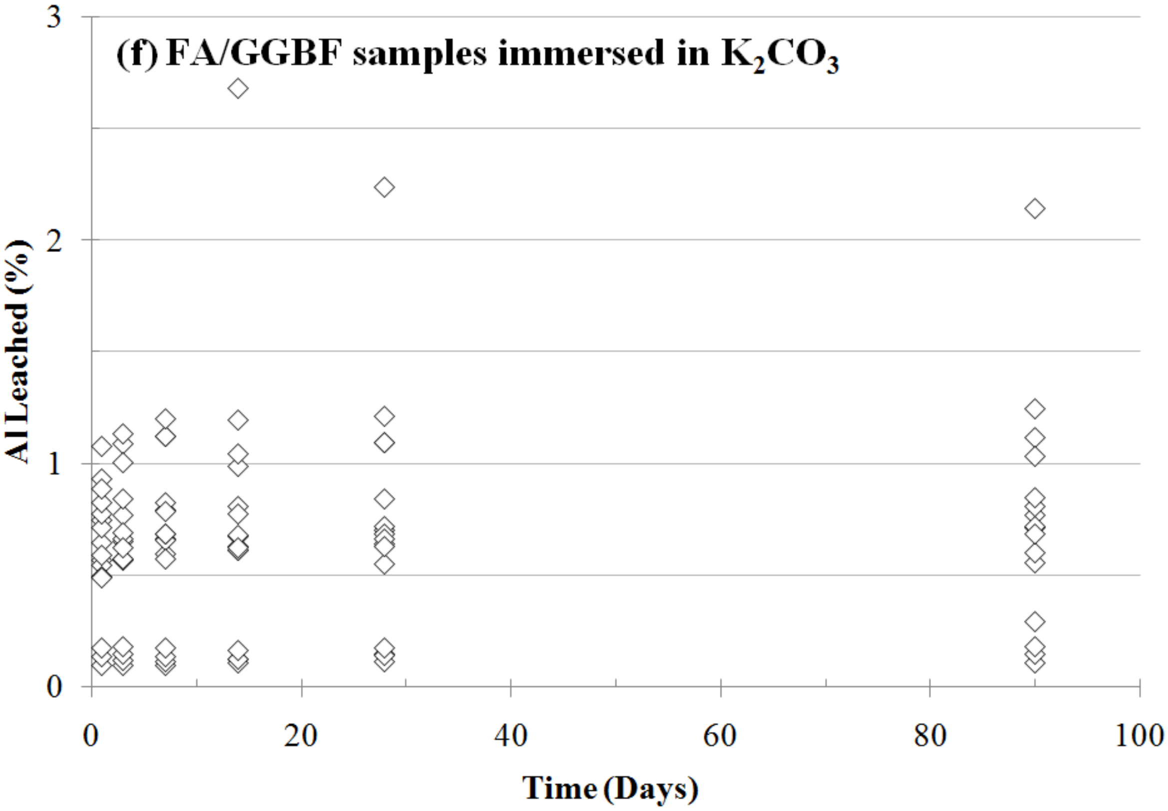

Figure 2. Leaching of Al from (a, b, c) the MK/GGBFS binders, and (d, e, f) the FA/GGBFS binders during 90 days of solvent exposure, (a, d) H_2O, (b, e) MEA, (c, f) K_2CO_3

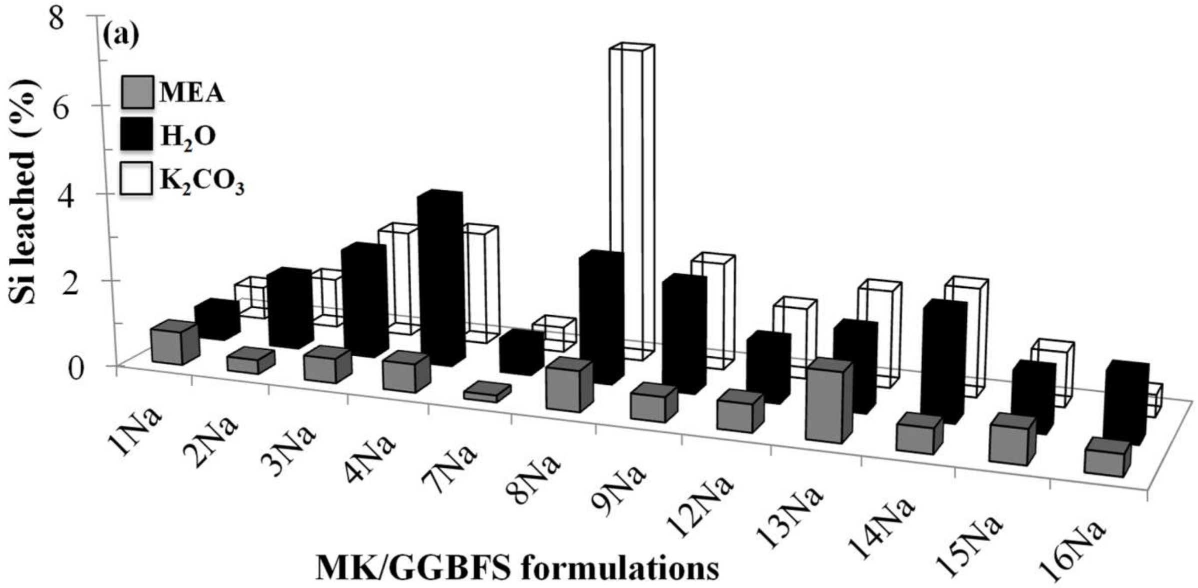

655

656

657

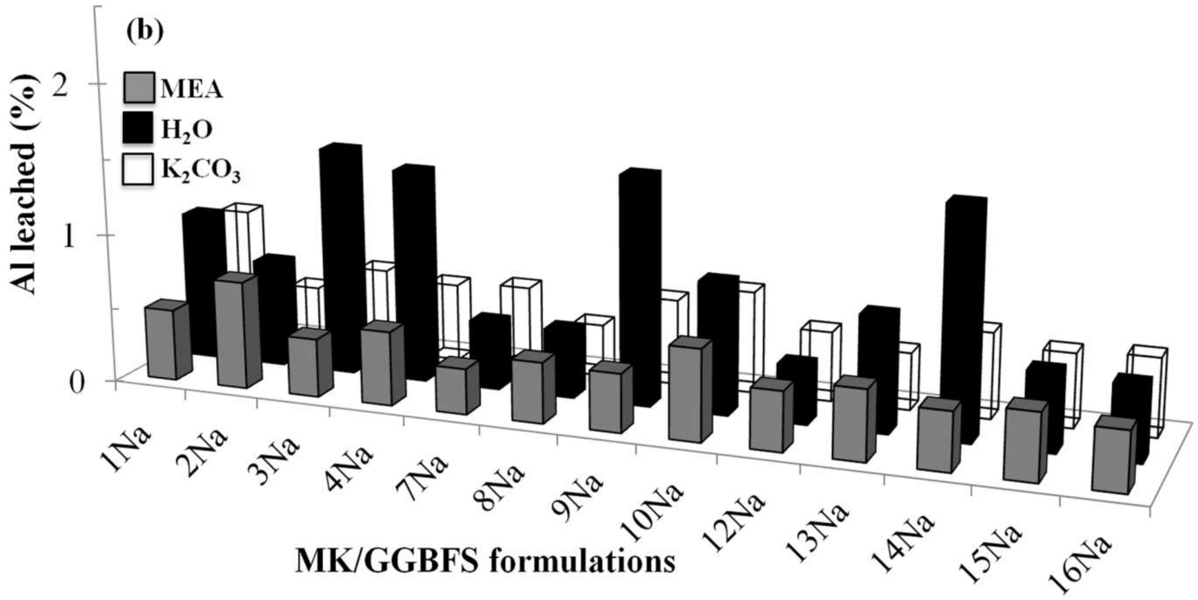

658

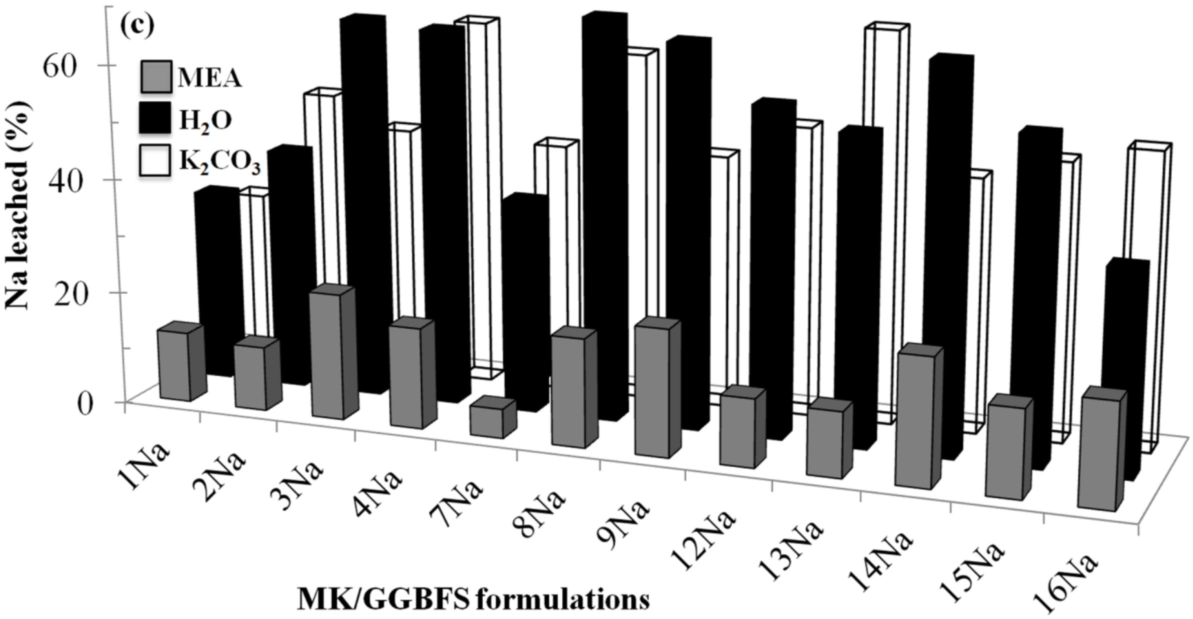
(c)
MEA
H_2O
K_2CO_3
Na leached (%)
0
20
40
60
1Na
2Na
3Na
4Na
7Na
8Na
9Na
12Na
13Na
14Na
15Na
16Na
MK/GGBFS formulations

659

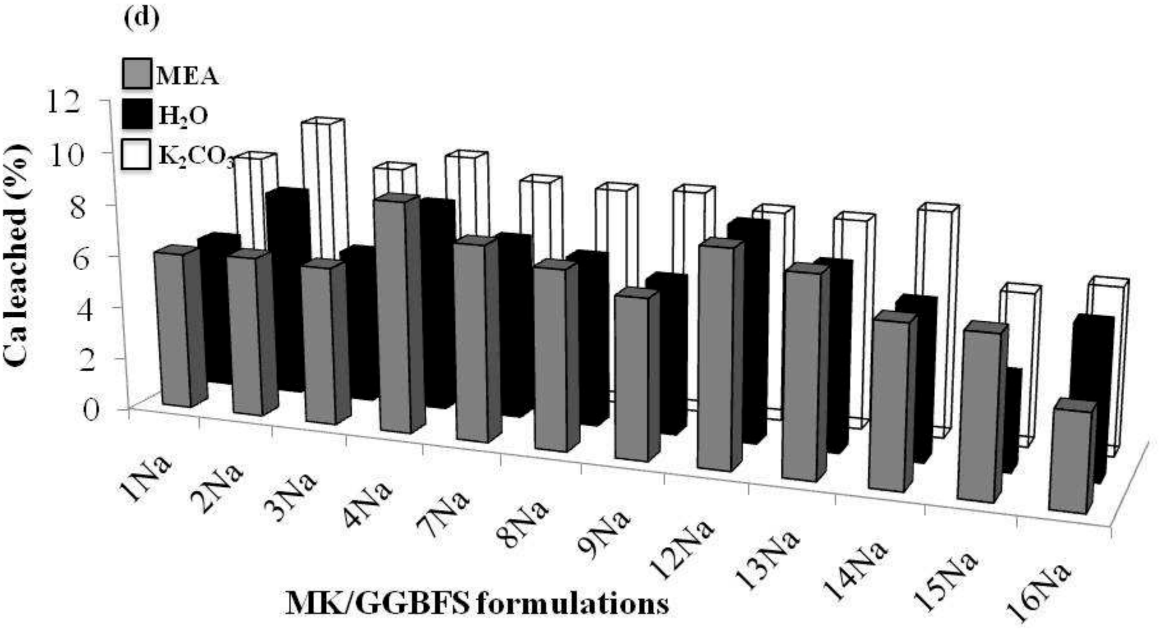
(d)
MEA
H_2O
K_2CO_3
Ca leached (%)
0
2
4
6
8
10
12
1Na
2Na
3Na
4Na
7Na
8Na
9Na
12Na
13Na
14Na
15Na
16Na
MK/GGBFS formulations

660

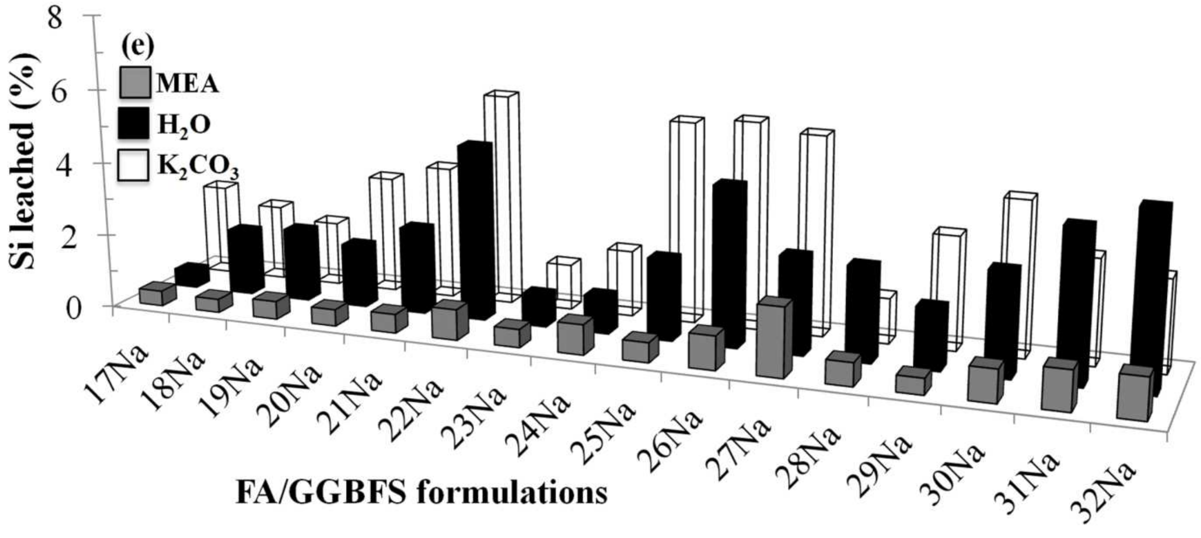
(e)
MEA
H_2O
K_2CO_3
Si leached (%)
8
6
4
2
0
17Na
18Na
19Na
20Na
21Na
22Na
23Na
24Na
25Na
26Na
27Na
28Na
29Na
30Na
31Na
32Na
FA/GGBFS formulations

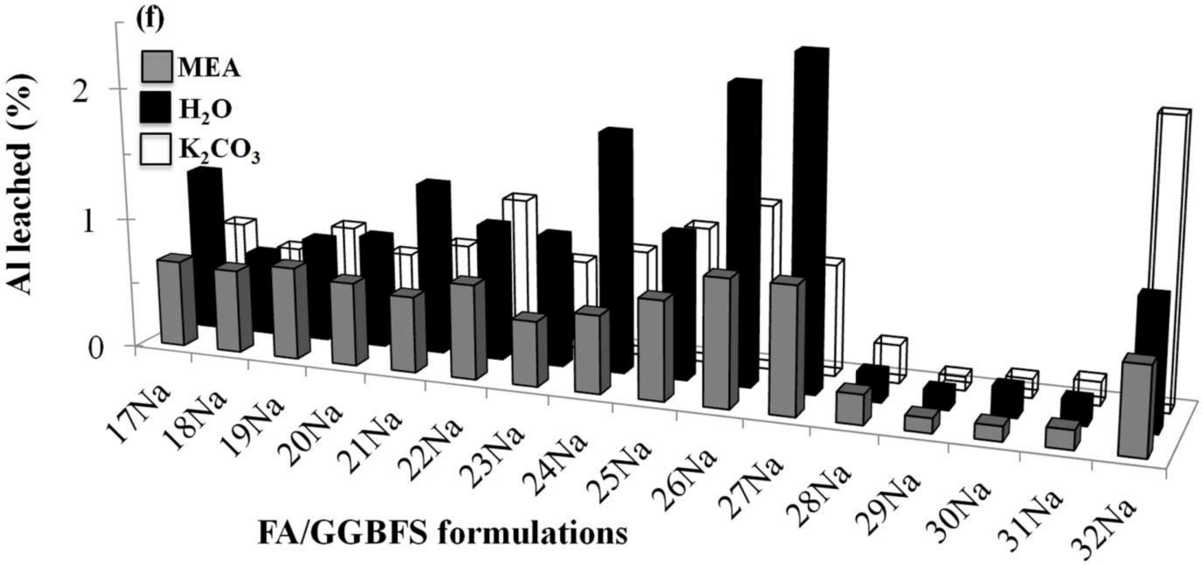
(f)
MEA
H_2O
K_2CO_3
Al leached (%)
2
1
0
17Na
18Na
19Na
20Na
21Na
22Na
23Na
24Na
25Na
26Na
27Na
28Na
29Na
30Na
31Na
32Na
FA/GGBFS formulations

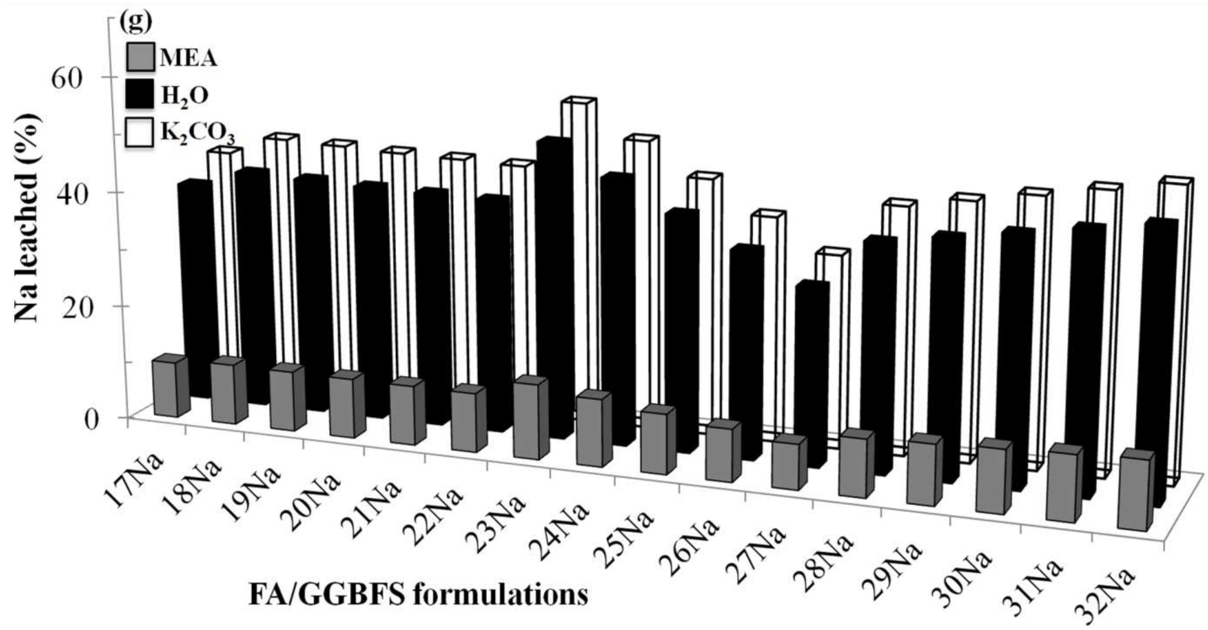

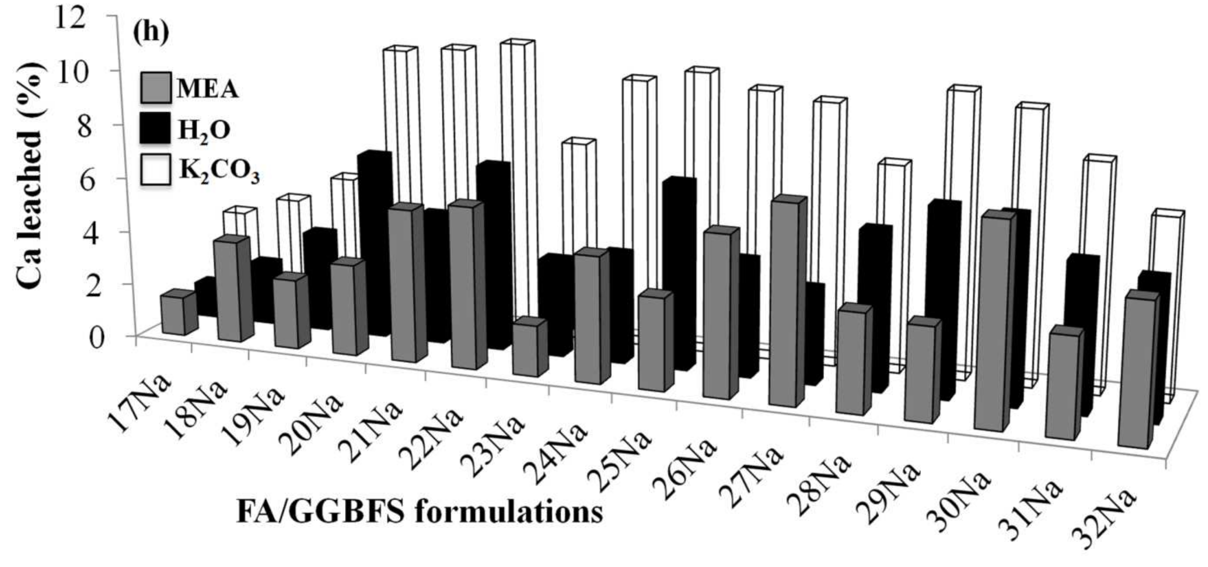

Figure 3. Leaching of (a) Si (b) Al (c) Na and (d) Ca from each of the MK/GGBFS geopolymer formulations, and of (e) Si, (f) Al, (g) Na and (h) Ca from each of the FA/GGBFS geopolymer formulations, following 90 days of solvent exposure.

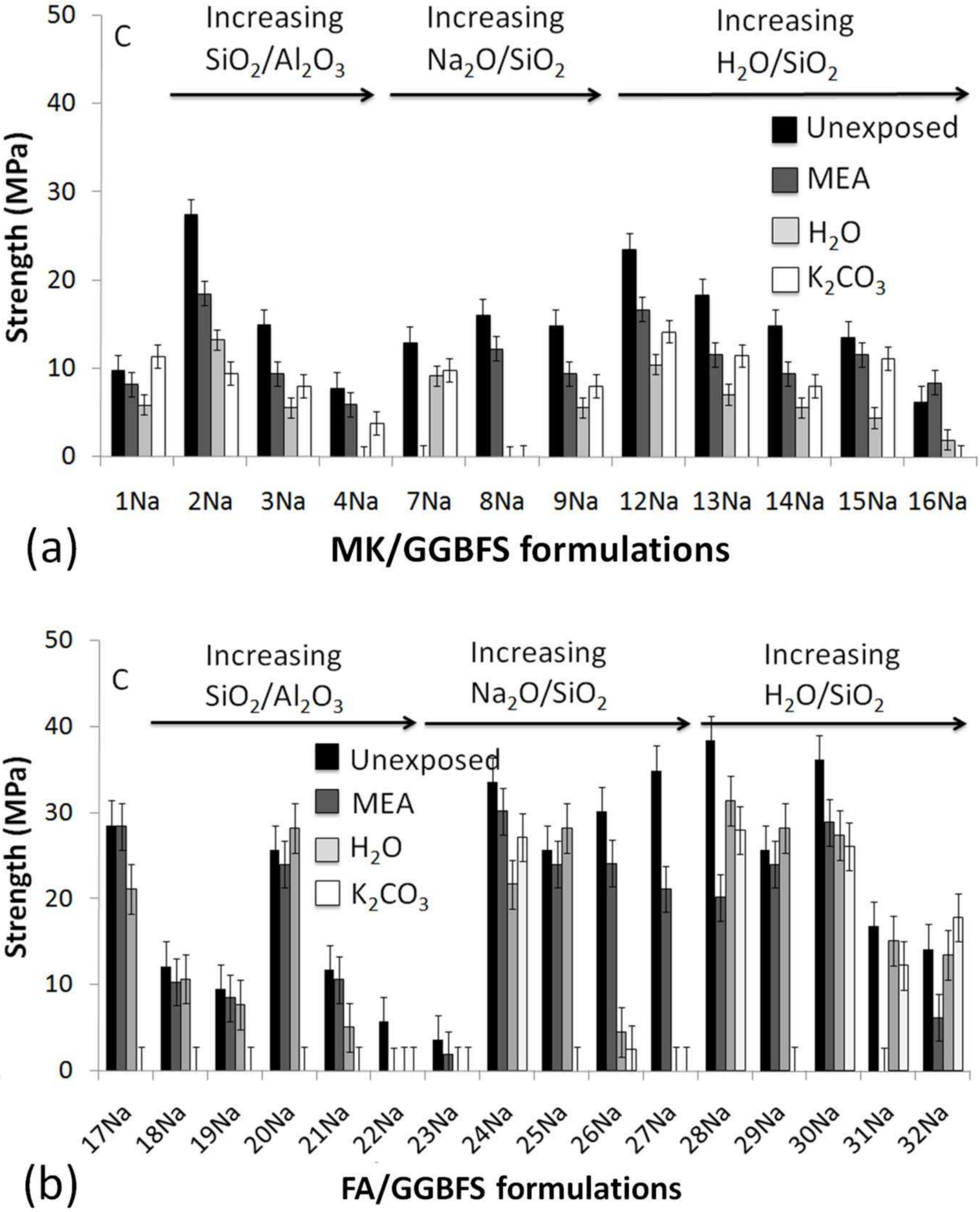

Figure 4. Compressive strengths of the (a) MK/GGBFS and (b) FA/GBFS formulations after 28days of unexposed aging and 28 days of solvent exposure. The formulation trends in each series are marked with arrows, and c denotes the control sample (without GGBFS) in each set.

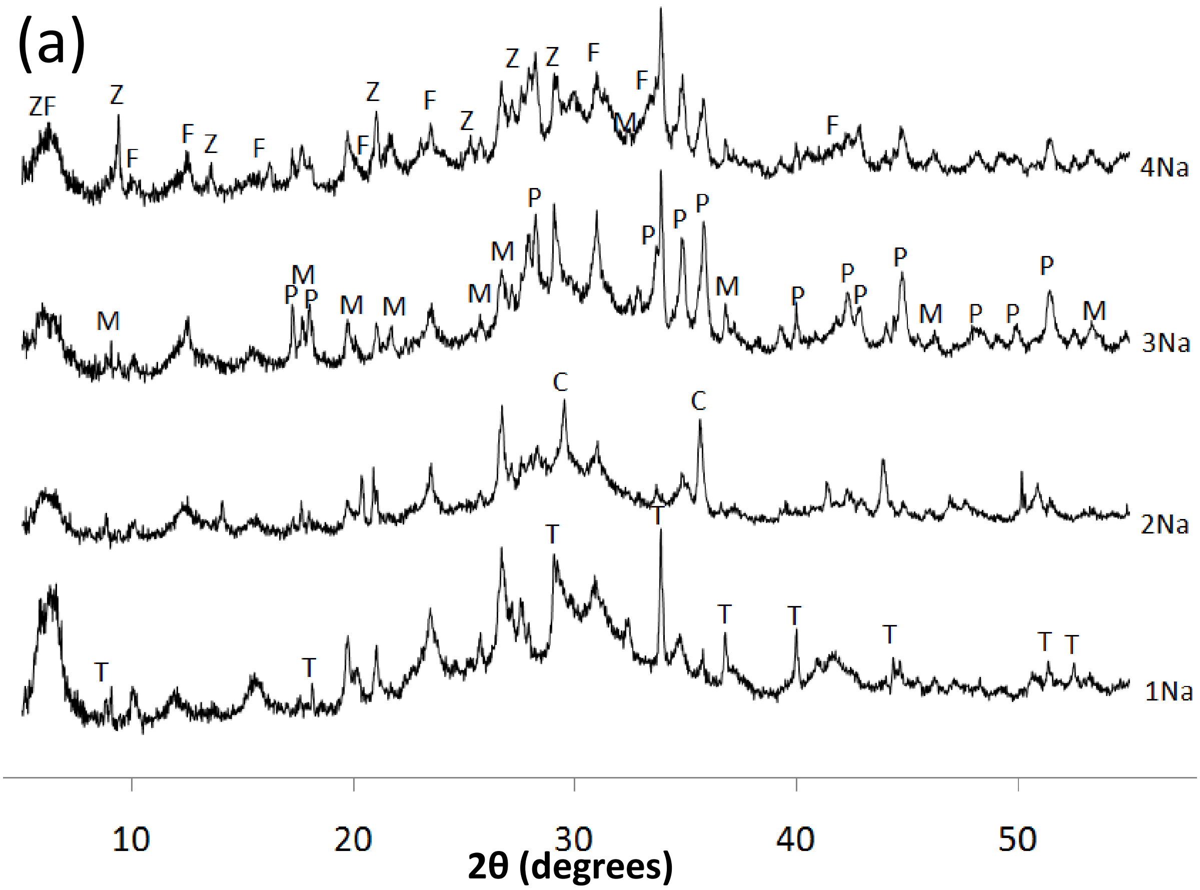
(a)
4Na
3Na
2Na
1Na
Z F Z F F Z F Z F F Z F Z Z F F M F
M P P M P M M M P P P P P M P P P P M P P P M
C C
T T T T T T T T T T
10
20
30
40
50
2θ (degrees)

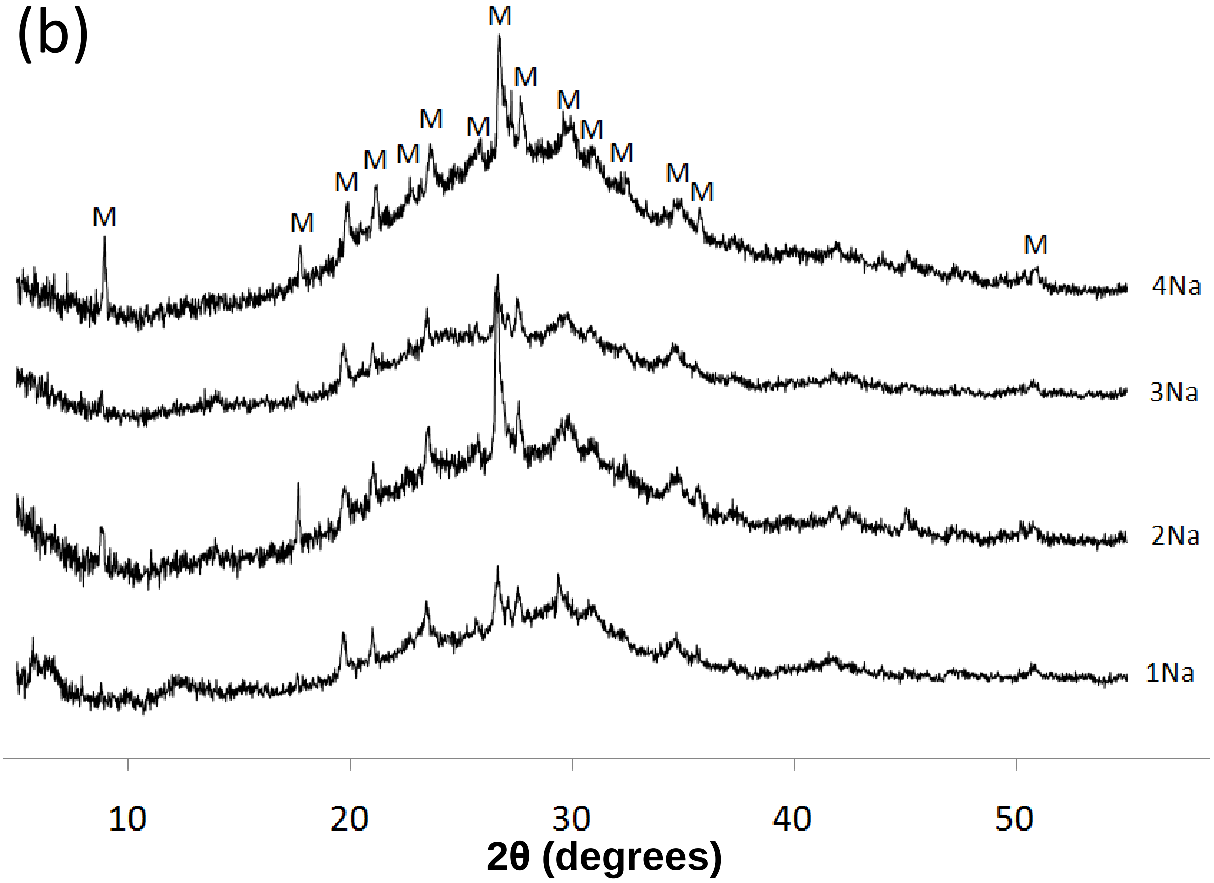

680
681

682

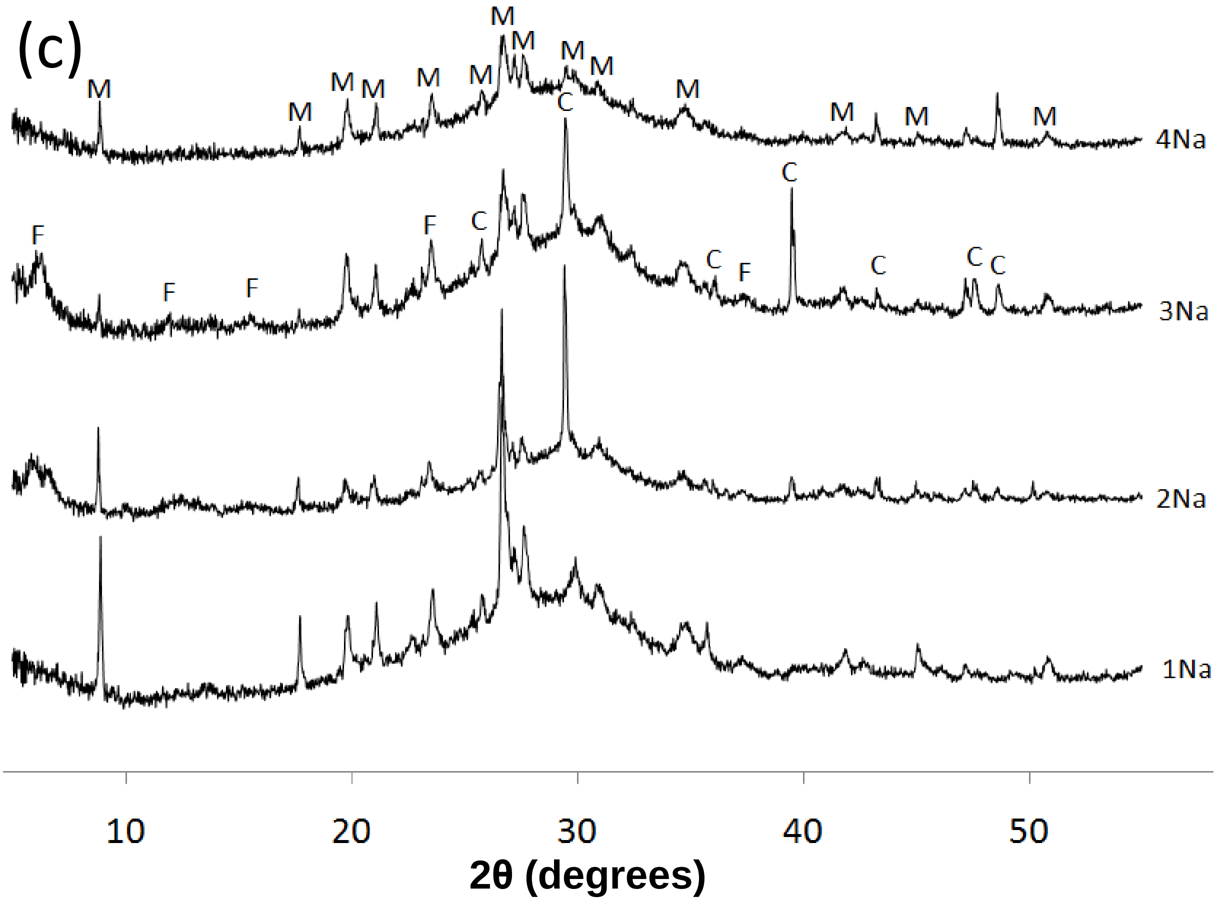
(c)
M
M
M
M
M
M
M
M
M
M
C
M
M
M
M
4Na
F
F
F
F
C
C
C
F
C
C
C
C
3Na
2Na
1Na
10
20
30
40
50
2θ (degrees)

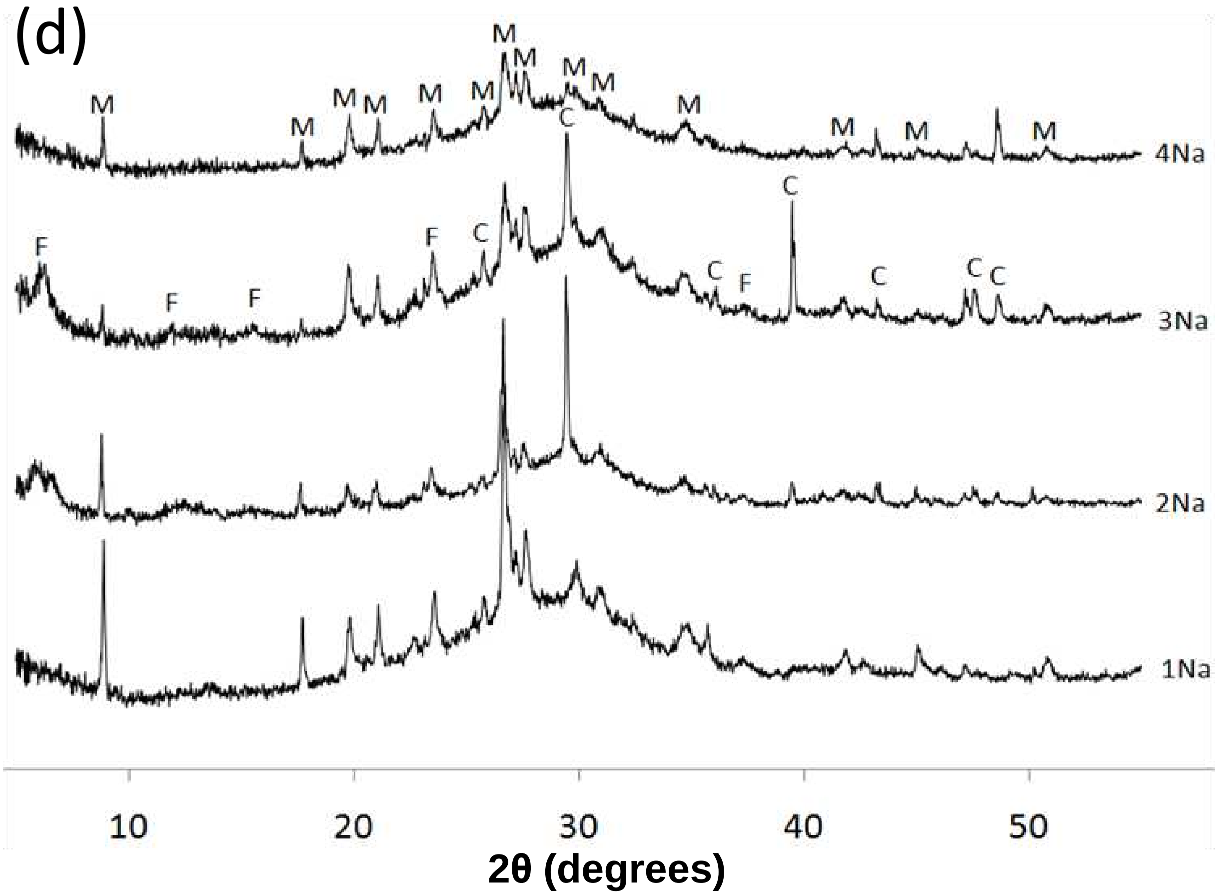

Figure 5. XRD traces of MK/GGBFS samples 1Na-4Na after (a) 7 days of curing and 90 days of aging, or 7 days of curing and 90 days of exposure to solvents: (b) MEA; (c) Milli-Q H_2O; (d) K_2CO_3. Phases marked are C: calcite, F: faujasite, M: muscovite, P: pirssonite, T: trona, Z: chabazite-Na.

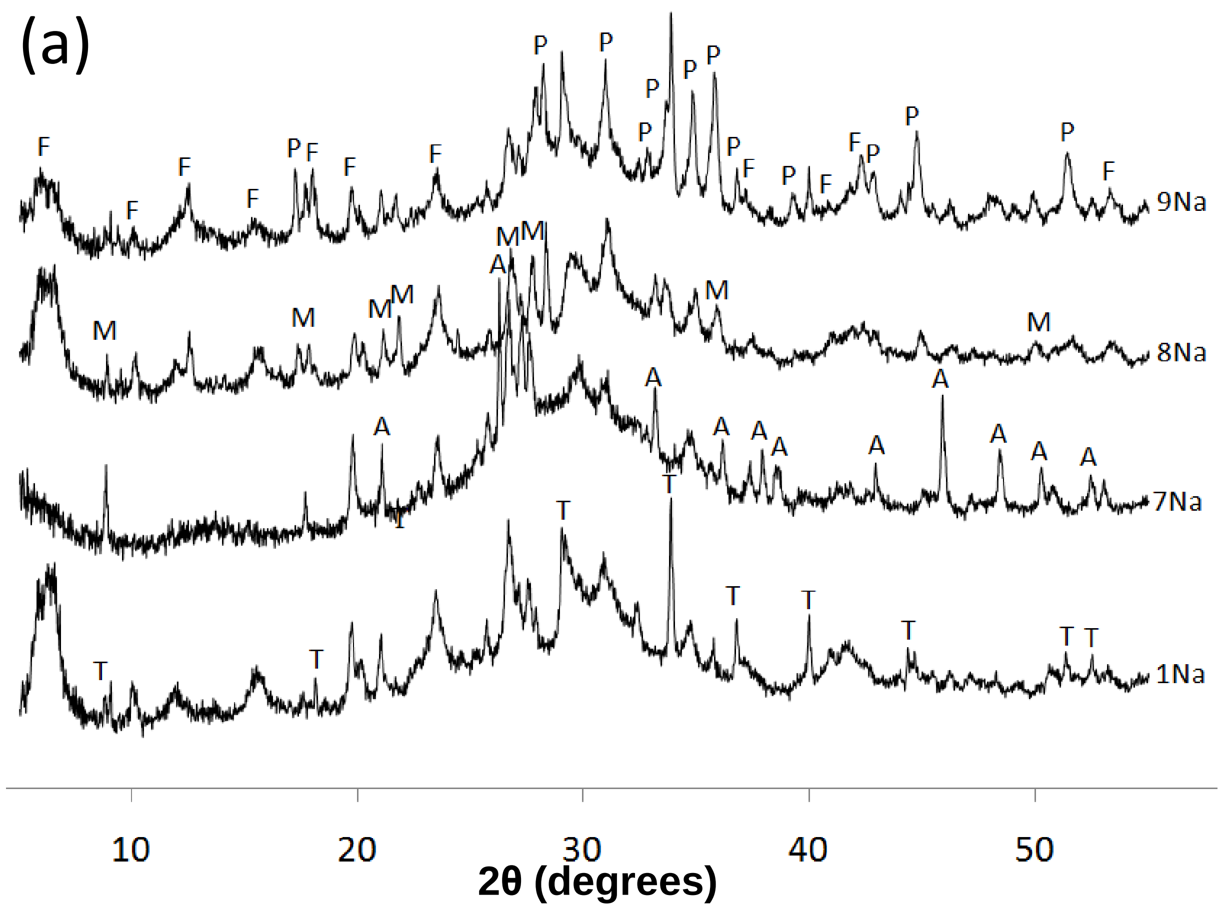
(a)
F
F
F
F
P
F
F
F
P
P
P
P
P
P
P
F
P
F
F
P
P
P
F
9Na
M
M
M
M
A
M
M
M
M
8Na
A
A
A
A
A
A
A
A
A
A
7Na
T
T
T
T
T
T
T
T
T
1Na
10
20
30
40
50
2θ (degrees)

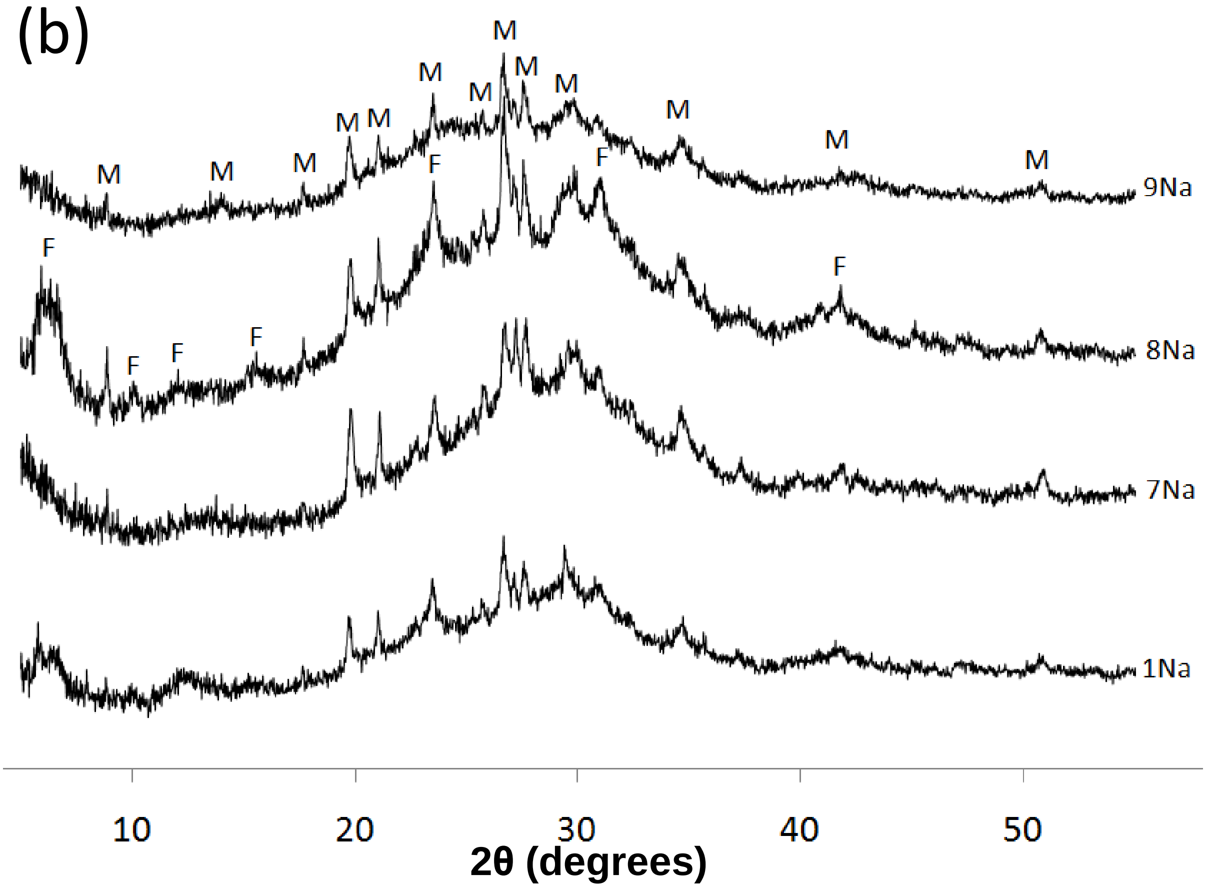
(b)
M
M
M
M
M
M
M
M
M
M
M
M
M
M
F
F
F
F
F
F
F
F
9Na
8Na
7Na
1Na
10
20
30
40
50
2θ (degrees)

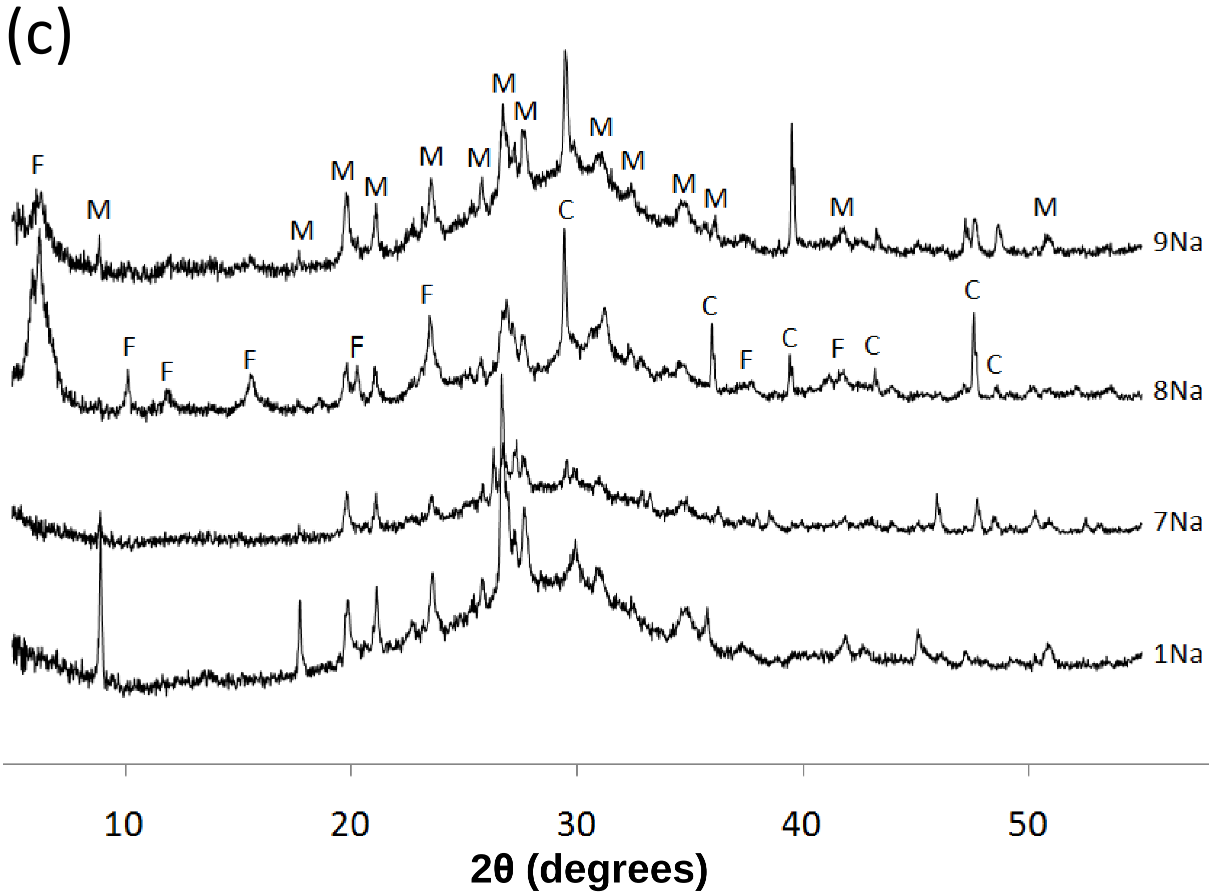
(c)
F
M
M
M
M
M
M
M
M
M
M
M
M
M
C
9Na
F
F
F
F
F
F
C
F
C
F
C
C
C
8Na
7Na
1Na
10
20
30
40
50
2θ (degrees)

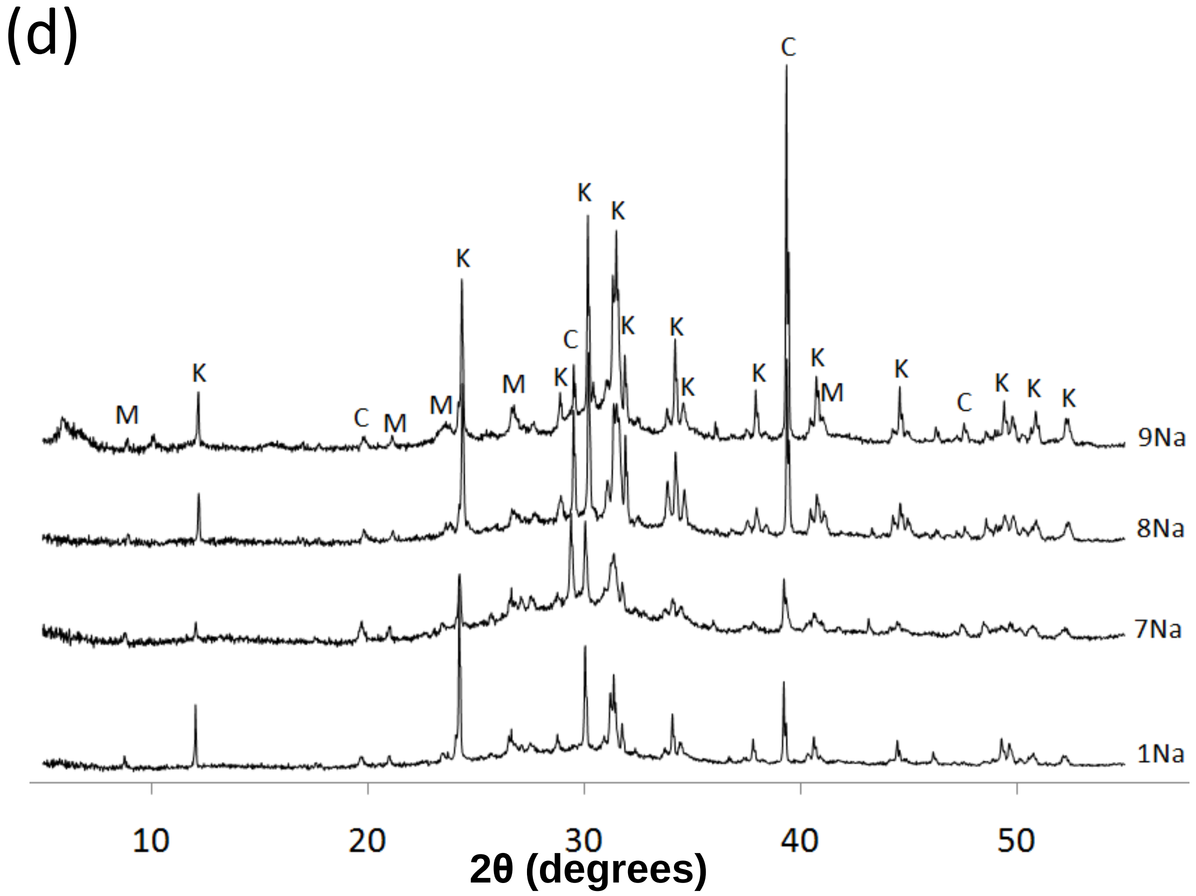

Figure 6. XRD traces of MK/GGBFS samples 1Na and 7Na-9Na after (a) 7 days of curing and 90 days of aging, or 7 days of curing and 90 days of exposure to solvents: (b) MEA; (c) Milli-Q H_2O; (d) K_2CO_3. Phases marked are A: aragonite, C: calcite, F: faujasite, K: kalcinite, M: muscovite, P: pirssonite, T: trona, Z: chabazite-Na.

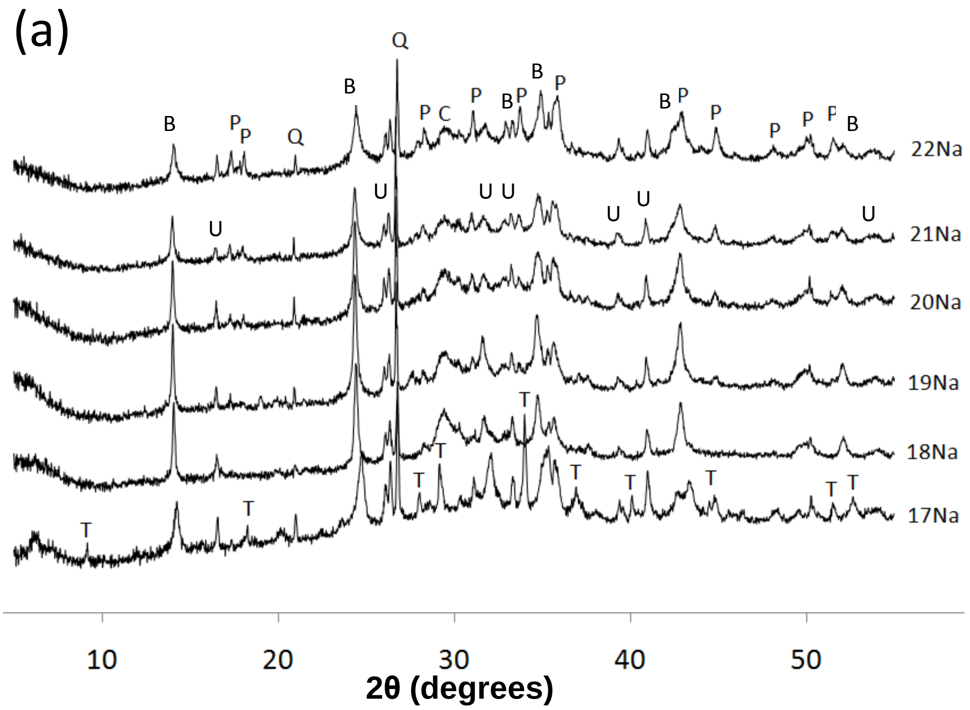
(a)
Q
B
B
P
B P
P
P C
B
P
P
Q
B P
P
P
P
P
B
22Na
U
U U
U
U
U
U
21Na
20Na
19Na
T
18Na
T
T
T
T
T
T
T
T
17Na
10
20
30
40
50
2θ (degrees)

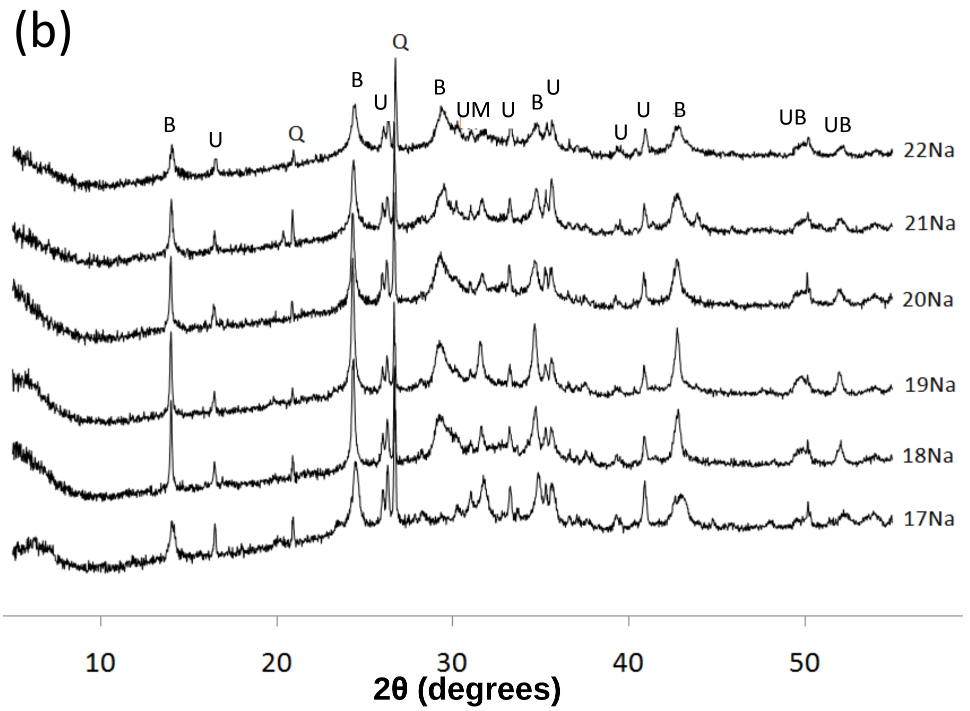
(b)
Q
B
U
B
UM
U
B
U
U
U
B
UB
UB
B
U
Q
22Na
21Na
20Na
19Na
18Na
17Na
10
20
30
40
50
2θ (degrees)

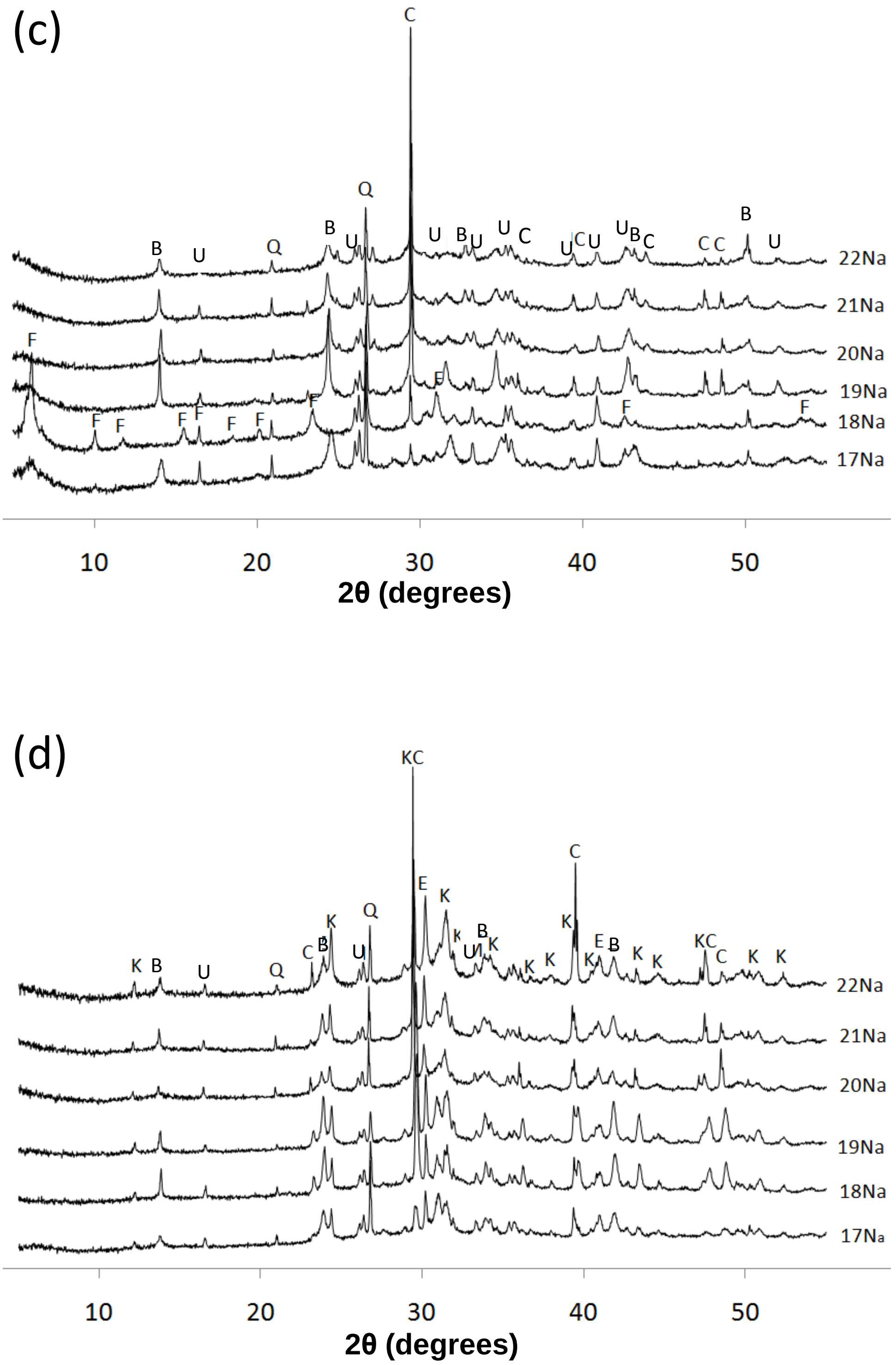

Figure 7. XRD traces of FA/GGBFS samples 17Na-22Na after (a) 7 days of curing and 90 days of aging, or 7 days of curing and 90 days of exposure to solvents: (b) MEA; (c) Milli-Q H_2O; (d) K_2CO_3. Phases marked are B: basic sodalite, U: mullite, Q: quartz, P: pirssonite, C: calcite, T: trona, F: faujasite, K: kalcinite, E: potassium carbonate.

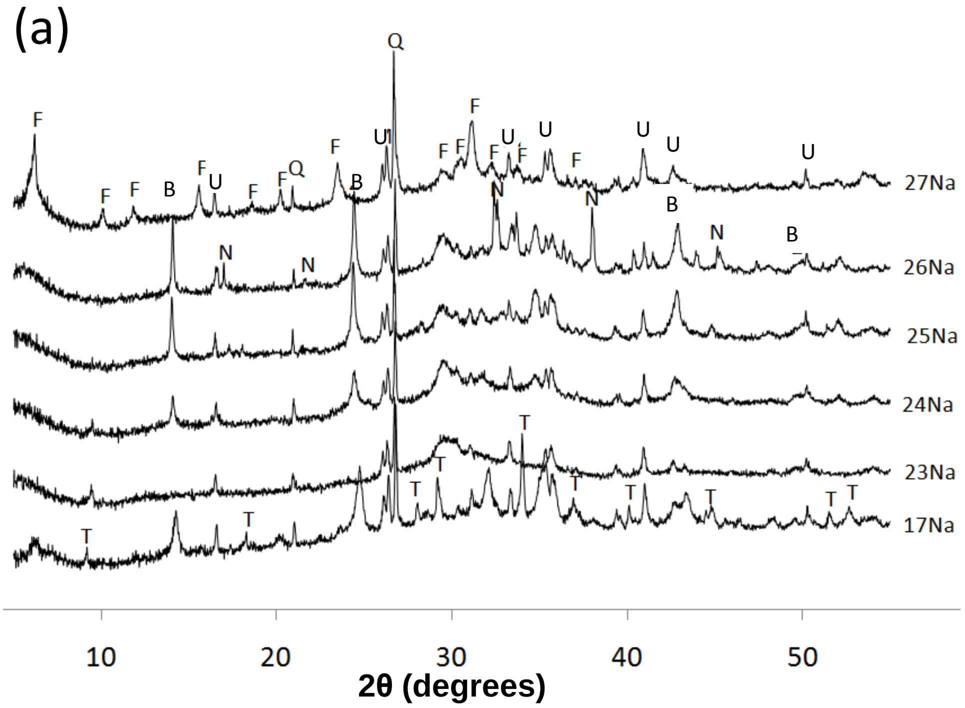
(a)
Q
F
U
B
N
T
27Na
26Na
25Na
24Na
23Na
17Na
10
20
30
40
50
2θ (degrees)

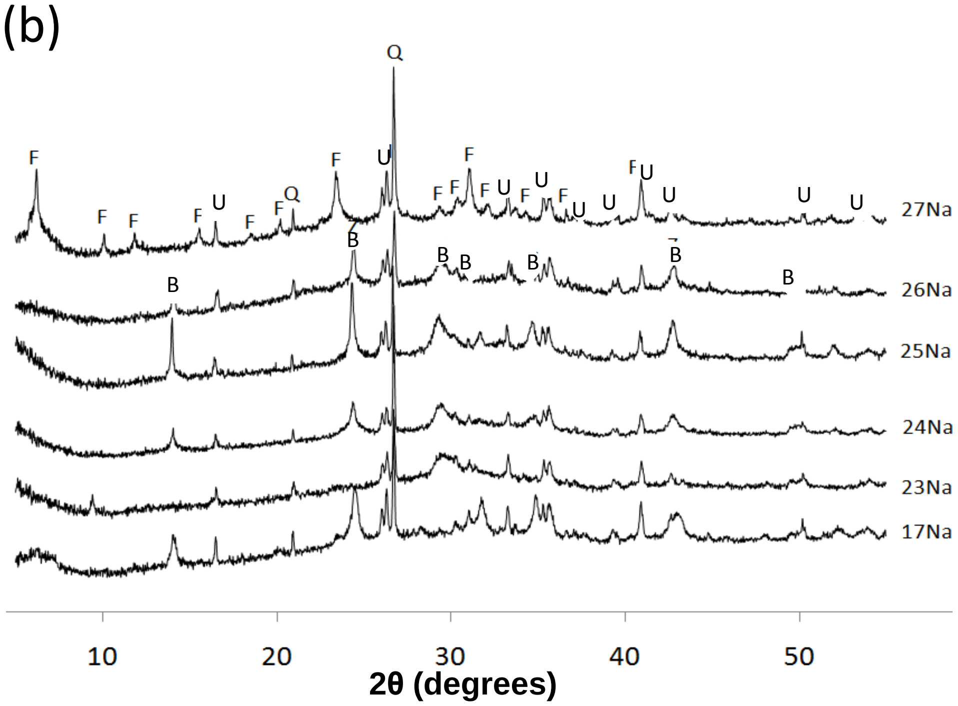
(b)
Q
F
U
B
27Na
26Na
25Na
24Na
23Na
17Na
10
20
30
40
50
2θ (degrees)

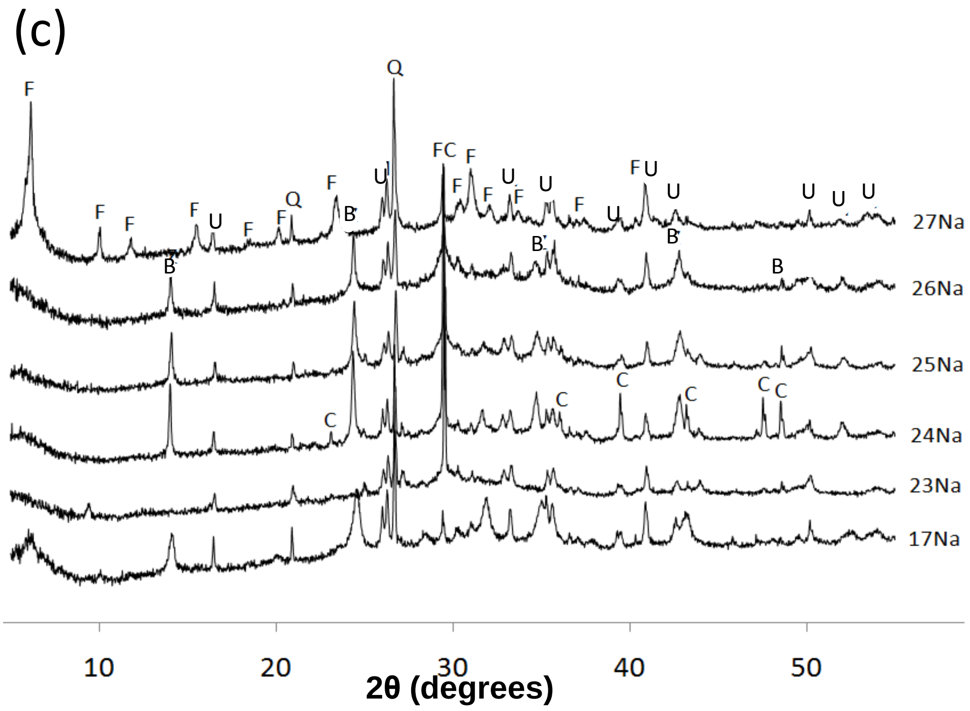

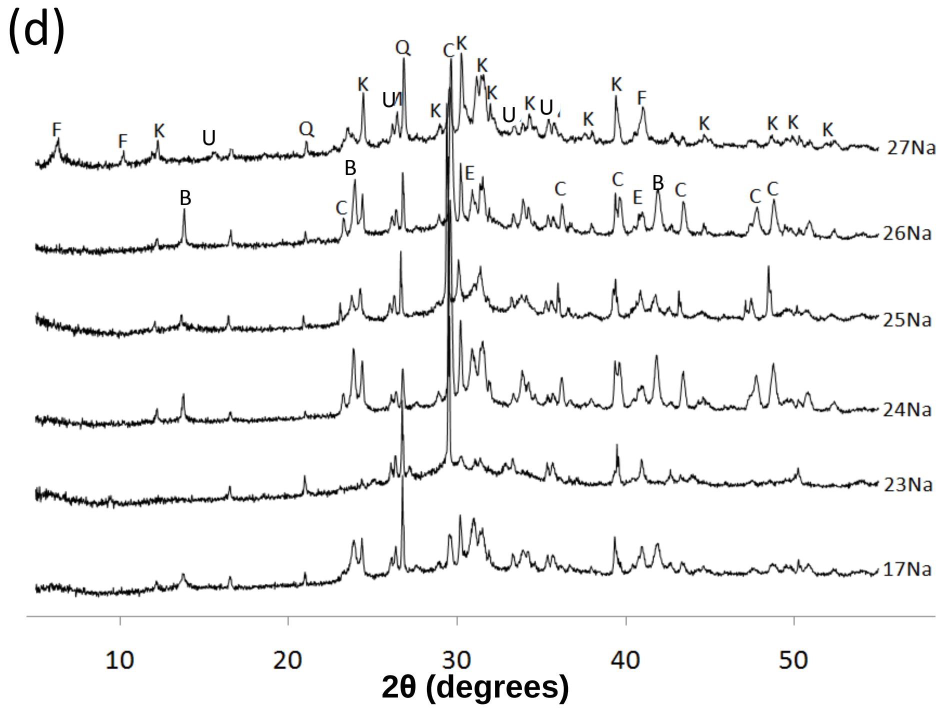

Figure 8. XRD traces of FA/GGBFS samples 17Na and 23Na-27Na after (a) 7 days of curing and 90 days of aging, or 7 days of curing and 90 days of exposure to solvents: (b) MEA; (c) Milli-Q H_2O; (d) K_2CO_3. Phases marked are B: basic sodalite, F: faujasite, Q: quartz, U: mullite, N: thermonatrite, T: trona, C: calcite, K: kalcinite, E: potassium carbonate.